NUMERICAL ANALYSIS OF NONLINEAR PNEUMATIC STRUCTURES

NSG 381

J. T. Oden

Associate Professor of Engineering Mechanics

W. K. Kubitza

Professor of Engineering Mechanics
University of Alabama Research Institute
University of Alabama in Huntsville
Huntsville, Alabama
U. S. A.

COLLOQUIUM ON PNEUMATIC STRUCTURES
Stuttgart, Germany
1967

NUMERICAL ANALYSIS OF NONLINEAR PNEUMATIC STRUCTURES

J. T. Oden* and W. K. Kubitza**

Abstract. This paper presents a systematic numerical procedure for the analysis of nonlinear behavior in general pneumatic structures. Recent advances in the application of the finite element method to the evaluation of finite strains and large displacements of elastic membranes are reviewed and extensions of the method to the analysis of large motions of reinforced fabrics, anisotropic metals, plastics, viscoelastic, and nonlinearly elastic materials are presented. Local yielding of metallic elasto-plastic membranes subjected to external pressure is also examined. By using linear displacement approximations and triangular finite elements, general nonlinear stiffness relations are derived. These lead to systems of nonlinear algebraic or ordinary differential equations in the generalized displacements and velocities which are solved numerically. Numerical results are included along with comparisons with available experimental data.

CONTENTS

---

* Associate Professor of Engineering Mechanics, University of Alabama Research Institute, Huntsville, Alabama, U. S. A.

**Professor of Engineering Mechanics, University of Alabama Research Institute, Huntsville, Alabama, U. S. A.

NOTATION

Indicial notation and the summation convention are used throughout this paper. Upper-case Latin indices indicate points in space and lower-case indices indicate elements of an array. In general, Greek indices are associated with local coordinate systems and range from 1 to 2. The following symbols are used:

$a_{i\alpha}$	Constants in displacement approximation
A, A_o	Area of deformed and undeformed element
b_{Ni}	Thermal load vector at node N
$c_{\alpha N}$	Node displacement coefficients
C, C_1, C_2	Material constants
d_i	Components of rigid-body translation
d_{ij}	Deformation rate tensor
e	Element identification index
E_e	Total number of finite elements
$E, E_1, E_2, \overline{E}$	Elastic moduli
$E_{\alpha\beta\lambda\mu}$	Multi-dimensional array of material constants
$f(\sigma_{ij})$	Yield surface
F_i	Body force per unit mass
$g_{\alpha\beta}$	A surface tensor
$G, \overline{G}, G_c$	Shear moduli
H	Heat input per unit mass
I_1, I_2, I_3	Strain invariants
m_{NM}, M_{NM}	Consistent mass matrices
n	Total number of nodes
p	Hydrostatic pressure
p_{Nke}	Generalized node forces of element e in local coordinates

P_{Nk}	Generalized node forces in global coordinates
q	External pressure
q_i, q_{Ni}	Components of heat flux
Q	Heat input
$Q_i, \bar{Q}_{ie}$	Element node forces due to q
u_i	Displacement components in local coordinates
u_{Nie}	Displacement of node N of element e in x_i direction in local coordinates
U	Total internal energy
U_{Ni}	Displacement of node N in Z_i-direction in global coodinates
v, v_o	Volumes of deformed and undeformed elements
W	Strain energy per unit of undeformed volume
x_{ie}	Local coordinates of element e
x_{Nie}	Local coordinates of node N of element e
y_{ie}	Local coordinates of deformed element e
y_{Nie}	Local coordinates of node N of element e after deformation
Z_i	Global coordinates
Z_{Ni}	Global coordinates of node N
β_{ije}	Orthogonal transformation matrix of element e
γ_{ij}	Lagrangian strain tensor
δ_{ij}	Kronecker delta
$\epsilon_{\alpha\beta}$	Two-dimensional permutation symbols
$\varkappa$	Kinetic energy
λ	Extension ratio
$\nu, \bar{\nu}, \nu_c$	Poisson's ratios
ξ	Internal energy per unit mass
ρ , ρ	Mass densities

$\sigma_{\alpha\beta}$	Stress tensor
$\overline{\sigma}_{\alpha\beta}$	Deviatoric stress tensor
Ω	Power of external forces
Ω_{NMe}	Multi-dimensional array

1. INTRODUCTION

1.1 Opening Remarks. Until recent years, the behavior of the majority of practical structures could be adequately described by linear theory. The deformations of most structural systems under working loads are usually so small as to be scarcely detectable with the unaided eye, and the stress-strain relations for such common materials as steel, aluminum, and even concrete can, for practical purposes, be treated as linear. Solutions of linear problems involving two and three-dimensional structures of general shape with complex boundary conditions, however, are often untractable by classical means and, even with the gross simplifications afforded by linear theories, many important problems remain unsolved.

With the bulk of the available methods of analysis being applicable to only linear systems and with these methods being often inadequate in the face of complex geometries, the engineer must look upon the recent trend toward the use of highly flexible pneumatic structures with some bewilderment. The behavior of inflatable pneumatic structures is inherently nonlinear: such structures often acquire their primary load-carrying capacity after undergoing deformations which, even under small pressures, may be so large that the original undeformed shape is unrecognizable. Strains appreciably greater than unity are not uncommon, and in such cases Hooke's law is not applicable. Moreover, the materials used to construct pneumatic structures are often anisotropic and nonlinearly elastic and, to further complicate matters, the directions and magnitudes of the applied loads change with the deformation. To emphasize this point, one need only refer to recent experimental studies on pneumatic structures wherein discrepancies on the order of 400 per cent were encountered when measured stresses were compared with those predicted by conventional linear theories.

It is clear that in order to accurately analyze general pneumatic structures one must turn to the general nonlinear theories of structural mechanics, many of which have long been regarded as only academic interest. Although only a small number of exact solutions to general nonlinear structural problems are available in the literature and although these, without exception, are concerned with only the most simple geometry, deformation, and loading, at least one can find here a rigorous and complete foundation on on which to base nonlinear analyses.

Fortunately, the trend toward the use of nonlinear structural systems has been accompanied by significant developments in both large-scale digital computers and general methods of numerical analysis. With the aid of these tools, many of the nonlinear structural theories can be employed to obtain useful information concerning the nonlinear behavior of pneumatic structures. Chief among the numerical schemes is the so-called finite element method wherein continuous structural systems are replaced by discrete models whose properties are consistent with the general field equations defining the behavior of the continuum. Notable progress has recently been made in applying this method to complex linear and nonlinear structural problems. A comprehensive review of applications of the finite element method to the analysis of nonlinear behavior in elastic membranes as well as several extensions of the method to the analysis of large deformations of elastic, elasto-plastic, and viscoelastic pneumatic structures is the subject of this paper.

1.2 Previous Related Work. Since 1950, the technical literature has contained numerous applications of the finite element approach to a wide variety of linear structural problems. Solutions to complex plane-stress, plate, and shell problems are available, along with several solutions to three-dimensional

elastic bodies. Applications to nonlinear problems, however, have been significantly less extensive. It appears that the first successful application of the finite element concept to the analysis of geometrically nonlinear problems was presented by Turner et al [1]. These authors solved certain nonlinear problems by dividing a large deformation into a number of steps. Within each step the structure is assumed to behave linearly and an instanteous (linear) stiffness matrix is computed in the deformed geometry. Argyris [2,3], Gallagher and Padlog [4], and Martin [5] were among several investigators who later applied this successive correction technique to large deflection and stability analyses. In these papers, the correction to the linear stiffness matrix is often referred to as the "geometric" stiffness of the structure, and it is ordinarily a function of the stresses associated with some reference equilibrium state. A survey of the literature using this approach is contained in the paper by Martin [5] and a general formula for geometric stiffness matrices was presented by Oden [6]. Following a different approach, Wissmann [7,8] obtained nonlinear finite element forumlations for certain problems involving large displacements but small strains of elastic structures.

Extensions of the finite element method to the analysis of finite deformations of elastic membranes and three-dimensional bodies were presented by Oden [9,10] and Oden and Sato [11]. Using a somewhat different approach, Becker [12] obtained a numerical solution to the problem of finite in-plane deformations of rubber sheets subjected to prescribed boundary displacements. These nonlinear formulations contain the linear stiffness matrices as special cases and lead to systems of nonlinear algebraic equations which must be solved numerically. At the same time, they are considerably more general than the successive correction methods mentioned earlier in that

they contain characteristics which are encountered only in highly nonlinear structural behavior.

1.3 Scope. In the discussion to follow, the basic philosophy of the finite element representation of flexible pneumatic structures is presented. General kinematic properties of thin membranes are cast in the form of algebraic equations defining the motion of an assembly of finite elements. The first law of thermodynamics is called upon to provide general relationships between kinematic and kinetic variables associated with the behavior of finite elements of arbitrary pneumatic structures. This leads to the general equation of motion of finite elements of thin membranes, and includes such properties as anisotropy, nonlinear viscoelasticity, thermoviscoelasticity, nonhomogenuity, and plasticity with no restrictions on the magnitudes of the deformations [Eq. (20)]. In order to obtain quantitative results, the general formulation is modified so that it applies to a number of important special cases. These include a review of the analysis of finite deformations of elastic membranes given in Refs. 9, 10, and 11 and applications to elastoplastic and viscoelastic structures. This is followed by discussions of procedures for assembling the finite elements, computing changes in loading due to deformation, and solution of the nonlinear equations generated in the analysis. Finally, the solutions of several representative problems are presented and numerical values are compared with available experimental data.

2. GEOMETRIC AND KINEMATIC CONSIDERATIONS

2.1 The Discrete Model. Classically, the analysis of continuous systems begins with investigations of the properties of small differential elements of the continuum under investigation. Relationships are established between

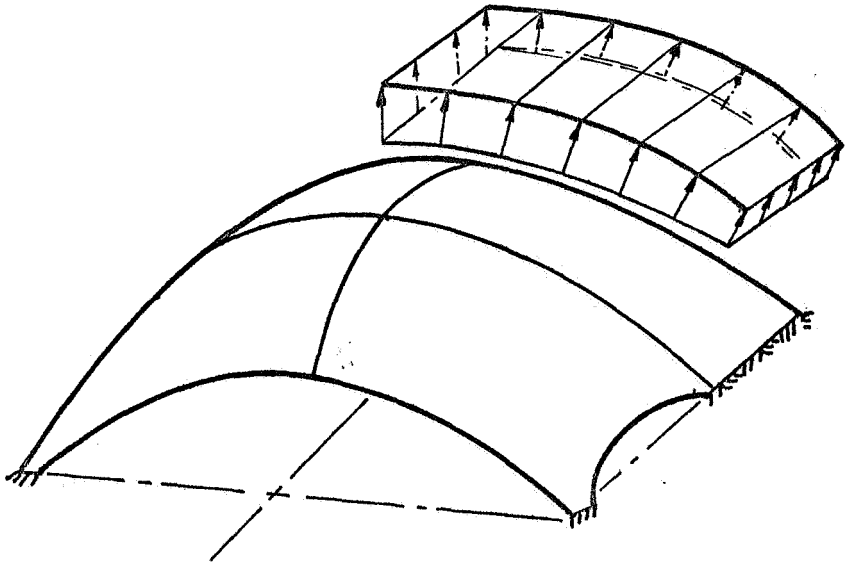

(a)

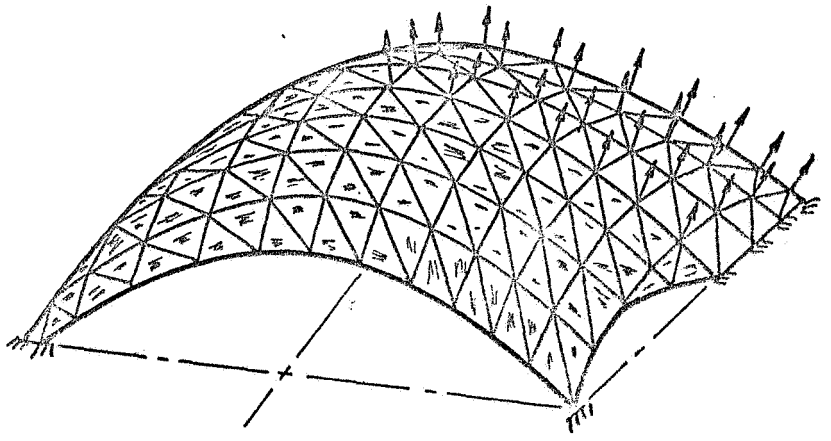

(b)

FIG. 1 Finite element representation of a pneumatic structure.

mean values of various quantities associated with the infinitesimal elements and partial differential equations governing the behavior of the entire domain are obtained by allowing the dimensions of the elements to approach zero as the number of elements becomes infinitely large. In contrast to this classical approach, in the present study we begin with investigations of the properties of elements of finite dimensions. We may employ equations of the continuous system in order to arrive at the properties of these elements; but the dimensions of the elements remain finite in the analysis, integrations are replaced by finite summations, and the differential equations of the continuous structure are replaced by systems of algebraic or ordinary differential equations. The continuous system with infinitely many degrees of freedom is thus represented by a discrete model which has finite degrees of freedom. Moreover, if certain kinematic conditions are satisfied, then, as the number of finite elements is increased and their dimensions are decreased, the behavior of the discrete system converges monotonically to that of the continuous system.

Consider, for example, the general pneumatic structure shown in Fig. 1a subjected to a general system of applied loads. To define the initial geometry of this system, a fixed rectangular cartesian coordinate system Z_1,Z_2,Z_3 is established which is referred to as the global reference frame. In general, an infinite number of coordinates Z_i are required to completely specify the initial configuration of the membrane; but in the present analysis, we reduce this continuously distributed system to a discrete one by representing the structure as an assembly of a finite number E_e of flat triangular elements, as indicated in Fig. 1b. The vertices of these triangular are referred to as the node points of the discrete model. Thus, if n denotes the total number of nodes in the system and if Z_{Ni}(N=1,2,...n;

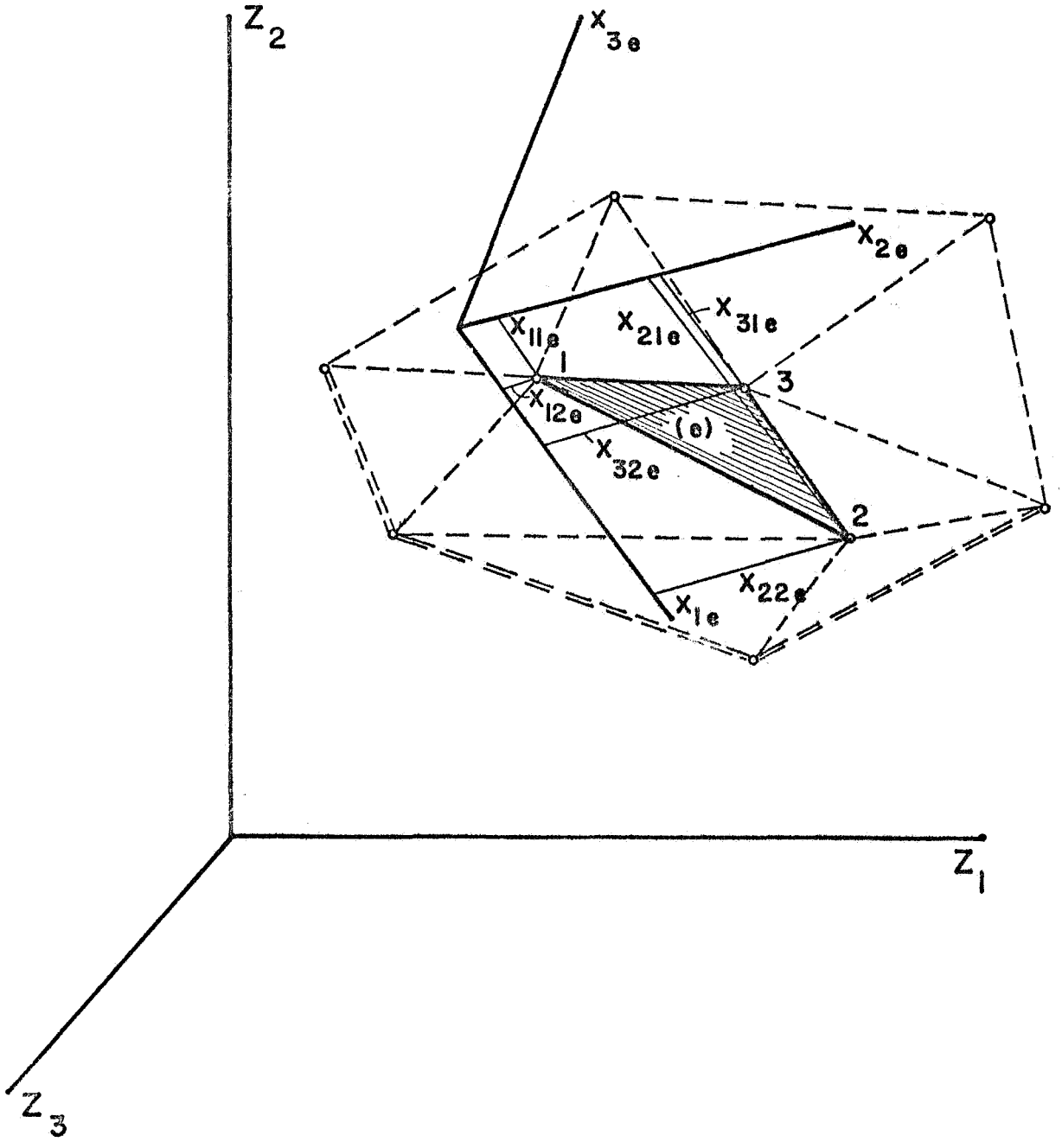

FIG. 2 Local and global coordinates of a typical finite element.

i=1,2,3) denote the global coordinates of a typical node N, then the set of numbers Z_{Ni} define the geometry of the discrete system.

In the finite element method, it is convenient to first describe the behavior of each element independently in terms of the displacements of its nodes; the entire set of elements is then connected together by establishing certain dependencies between appropriate node displacements. Toward this end, fixed local coordinate systems x_{ie}(i=1,2,3; e=1,2,...,E_e) are established in the neighborhoods of each finite element. The quantities x_{ie} are referred to as the local coordinates of element e. For simplicity, it is assumed that the middle surface of each element e lies in the x_{1e},x_{2e} - plane of its local coordinate system. Following a procedure similar to that used for global coordinates, the local coordinates of a typical node N of element e are denoted x_{Nie}(N,i = 1,2,3; e=1,2,...,E_e) where, due to our particular choice of coordinates, $x_{N3e} = 0$. These coordinates are illustrated in Fig. 2.

A rigid rotation of a typical local system x_{ie} into a local system $\bar{x}_{ie}$ whose coordinate lines are parallel to the corresponding global coordinate axes, is accomplished by the orthogonal transformation

$$\bar{x}_{ie} = \beta_{ji\underline{e}} x_{j\underline{e}} \quad \text{(no sum on e)} \tag{1}$$

where β_{jie} is the direction cosine of the angle between Z_i (or $\bar{x}_{ie}$) and x_{je}. The local coordinates of node N parallel to the global coordinates are denoted $\bar{x}_{Nie}$.

2.1 Strains and Displacements. In order that the present discussion be self-contained, we reproduce in this section the derivation of the general nonlinear stiffness relations for finite elements of membrane structures [9,10,11]. For the present, we confine our attention to a typical finite element and we temporarily drop the element identification index e for clarity.

Under a general deformation, line elements originally straight in the undeformed structure become curved lines in the deformed structure. Hence, an initially flat element is generally deformed into a curved surface. However, if the node points are selected sufficiently close of one another, node lines in the deformed configuration are closely approximated by straight-line segments. Then plane elements remain plane after the deformation. This is equivalent to assuming that the displacement fields within each element are linear functions of the local coordinates of the element.

Assuming, for simplicity, that the element is initially in the x_1, x_2 plane and denoting by u_i the components of displacement referred to the local coordinates of the element under consideration, it follows that

$$u_i = d_i + a_{i\alpha}x_\alpha \quad i = 1, 2, 3 \quad \alpha = 1, 2 \tag{2}$$

where d_i are the rigid-body translations of the element and the $a_{i\alpha}$ are undetermined constants. By evaluating Eq. (2) at each of the three nodes of the element, we arrive at nine simultaneous equations in the nine unknowns d_i, $a_{i\alpha}$. Solving these we find that

$$d_i = k_N u_{Ni} \tag{3}$$

and

$$a_{i\alpha} = c_{\alpha N} u_{Ni} \tag{4}$$

where u_{Ni} is the displacement of node N in the x_i direction,

$$\begin{aligned} k_1 &= \frac{1}{2A_o}(x_{21}x_{32} - x_{31}x_{22}) \\ k_2 &= \frac{1}{2A_o}(x_{12}x_{31} - x_{11}x_{32}) \\ k_3 &= \frac{1}{2A_o}(x_{11}x_{22} - x_{12}x_{31}) \end{aligned} \tag{5}$$

and

$$c_{\alpha N} = \frac{1}{2A_o}\begin{bmatrix} x_{22} - x_{32} & x_{32} - x_{12} & x_{12} - x_{22} \\ x_{31} - x_{21} & x_{11} - x_{31} & x_{21} - x_{11} \end{bmatrix} \tag{6}$$

In these equations, $x_{N\alpha}$ ($N = 1, 2, 3$; $\alpha = 1, 2$) are the local coordinates of node N and A_o is the area of the undeformed triangle.

Substituting Eqs. (3) and (4) into Eq. (2) gives

$$\begin{aligned} u_i &= k_N u_{Ni} + c_{\alpha N} u_{Ni} x_\alpha \\ \alpha &= 1,2 \; ; \quad N,i = 1,2,3 \end{aligned} \tag{7}$$

According to Green and Adkins [13], the Lagrangian strain tensor for a thin membrane is given by

$$\begin{aligned} \gamma_{\alpha\beta} &= \frac{1}{2}\left(\frac{\partial u_\alpha}{\partial x_\beta} + \frac{\partial u_\beta}{\partial x_\alpha} + \frac{\partial u_i}{\partial x_\alpha}\frac{\partial u_i}{\partial x_\beta}\right) \\ \gamma_{\alpha 3} &= 0 \\ \gamma_{33} &= \frac{1}{2}(\lambda^2 - 1) \end{aligned} \tag{8}$$

where λ is a scalar function representing the extension ratio at the middle surface in a direction normal to the surface. For very thin membranes, the strains are essentially uniform over the thickness and

$$\lambda = \frac{h}{h_o} \tag{9}$$

where h_o and h are the thicknesses of the membrane before and after deformation respectively.

Introducing Eq. (7) into Eqs. (8), we find for the strains in the discrete system

$$\begin{aligned} \gamma_{\alpha\beta} &= \frac{1}{2}(c_{\alpha N} u_{N\beta} + c_{\beta N} u_{N\alpha} + c_{\alpha N} c_{\beta M} u_{Ni} u_{Mi}) \\ \gamma_{\alpha 3} &= 0 \qquad \gamma_{33} = \frac{1}{2}(\lambda^2 - 1) \\ \alpha,\beta &= 1,2 \qquad M,N,i = 1,2,3 \end{aligned} \tag{10}$$

The strain components are thus constant throughout the finite element and, since they are determined from prescribed displacement fields, they automatically satisfy the equations of compatibility throughout the element. Note also that the components of displacement along the boundaries of an element are linear functions of the local coordinates. Since each edge contains two nodes and since the displacements are linear along each edge, it follows that the displacements are continuous across element boundaries. These properties of the approximation insure monotonic convergence of the solutions as the finite-element representation is refined.

Three invariants can be formed from every symmetric second-order tensor. In the analysis of deformable membranes, it is convenient to form the invariants of the deformation tensor $(\delta_{ij} + 2\gamma_{ij})$, where δ_{ij} is the Kronecker delta ($\delta_{ij} = 1$ for $i = j$ and $\delta_{ij} = 0$ for $i \neq j$). These invariants are given by the formulas

$$\begin{aligned} I_1 &= \lambda^2 + 2(1 + \gamma_{\alpha\alpha}) \\ I_2 &= -\lambda^4 + \lambda^2 I_1 + \frac{1}{\lambda^2} I_3 \\ I_3 &= \lambda^2 \phi \end{aligned} \tag{11}$$

where

$$\phi = 1 + 2\gamma_{\alpha\alpha} + 2\epsilon_{\alpha\beta}\epsilon_{\lambda\mu}\gamma_{\alpha\lambda}\gamma_{\beta\mu} \tag{12}$$

and $\epsilon_{\alpha\beta}$, $\epsilon_{\lambda\mu}$ are the two-dimensional permutation symbols ($\epsilon_{12} = 1$, $\epsilon_{21} = -1$, $\epsilon_{11} = \epsilon_{22} = 0$).

3. THERMODYNAMICS OF FINITE ELEMENTS

3.1 The General Equation of Motion of a Finite Element. Having defined the discrete system in the previous section, we now turn to certain fundamental principles of mechanics in order to obtain general equations of motion for a finite element. We begin with the first law of thermodynamics:

$$\dot{\mathcal{K}} + \dot{U} = \Omega + Q \tag{13}$$

where $\dot{\mathcal{K}}$ is the time rate of change of kinetic energy, $\dot{U}$ is the time rate of change of internal energy, Ω is the power developed by the external forces, and Q is the heat input. By definition,

$$\begin{aligned} \mathcal{K} &= \frac{1}{2}\int_V \rho \dot{u}_i \dot{u}_i dv \\ U &= \int_V \rho \xi \, dv \\ \Omega &= \int_V F_i \dot{u}_i \rho dv + \int_S S_i \dot{u}_i \, ds \\ Q &= \int_V \rho H \, dv + \int_S q_i n_i \, ds \end{aligned} \tag{14}$$

In these equations, ρ is the mass density, dv is the differential volume, $\dot{u}_i$ are the velocity components, ξ is the internal energy per unit mass, F_i are the body forces per unit mass, S_i are the surface tractions per unit of surface area s, H is the heat input per unit mass, q_i are the components of heat flux, and n_i are the components of a unit vector normal to the boundary surfaces of the element.

Through arguments similar to those used in obtaining Eq. (7), it is found that

$$\dot{u}_i = \frac{\partial u_i}{\partial t} = k_N \dot{u}_{Ni} + c_{\alpha N} \dot{u}_{Ni} x_\alpha \tag{15}$$

and

$$q_i = k_N q_{Ni} + c_{\alpha N} q_{Ni} x_\alpha \tag{16}$$

where u_{Ni} is the velocity of node N in direction i and q_{Ni} is the heat flux at node N in direction i. Moreover, if ρ_o, v_o and ρ, v denote the mass densities and the volumes of the finite element in the undeformed and the deformed states respectively, then according to the principle of conservation of mass,

$$\rho_o v_o = \rho v \tag{17}$$

Introducing Eqs. (15), (16), and (17) into Eqs. (14) and simplifying, we find

$$\begin{aligned} \mathcal{K} &= \frac{1}{2} m_{NM} \dot{u}_{Ni} \dot{u}_{Mi} \\ U &= \int_{v_o} \rho_o \xi \, dv_o \\ \Omega &= p_{Ni} \dot{u}_{Ni} \\ Q &= b_{Ni} q_{Ni} + \rho_o v_o H \end{aligned} \tag{18}$$

where

$$\begin{aligned} m_{NM} &= \int_{v_o} \rho_o (k_N + c_{\alpha N} x_\alpha)(k_M + c_{\beta M} x_\beta) dv_o \\ p_{Ni} &= \int_{v_o} F_i (k_N + c_{\alpha N} x_\alpha) \rho_o dv_o + \int_s S_i (k_N + c_{\alpha N} x_\alpha) ds \\ b_{Ni} &= \int_s (k_N + c_{\alpha N} x_\alpha) n_i \, ds \end{aligned} \tag{19}$$

The array m_{NM} is the so-called consistent mass matrix for the finite element and the quantities p_{Ni} are the components of generalized force corresponding to the generalized displacements u_{Ni}. Physically, p_{Ni} is the generalized force at node N in direction i. The quantities b_{Ni} are the generalized thermal gradients usually referred to as thermal loads. Note that the heat input H is regarded as a constant for each finite element.

Introducing Eqs. (18) into Eq. (13), we obtain the general result

$$m_{NM} \ddot{u}_{Ni} \dot{u}_{Mi} + \int_{v_o} \rho_o \dot{\xi} \, dv_o = p_{Ni} \dot{u}_{Ni} + b_{Ni} q_{Ni} + \rho_o v_o H \tag{20}$$

where $\ddot{u}_{Ni}$ are the components of acceleration of the nodes. This relation represents the most general discrete representation of the equations of motion for a finite element of a continuous media. It is applicable to the

analysis of large deformations of nonlinearly elastic, plastic, viscoelastic, and thermoviscoelastic media since no restrictions have as yet been placed on the constitutive equations for the material of which the element is composed or the magnitude of the deformation. The second and third terms on the right-hand side of Eq. (20) represent thermal effects on the motion of the element. The rate of change of internal energy $\dot{\xi}$ is, in general, also a function of the heat flux and the temperature gradients. These effects will not be considered further in this discussion; for our purposes, it suffices to merely point out that thermal effects can be easily included in the analysis by retaining the terms $b_{Ni}q_{Ni}$ and $\rho_o v_o H$ in Eq. (20) and by introducing, in addition to a constitutive equation involving the stress, a second constitutive equations which relates heat flux to thermal gradients, deformation rates, strains, etc. Thus, with thermal effects omitted, Eq. (20) reduces to

$$p_{Ni}\dot{u}_{Ni} = m_{NM}\ddot{u}_{Mi}\dot{u}_{Ni} + \int_{V_o} \rho_o \dot{\xi}\, dv_o \tag{21}$$

3.2 Internal Energy. To apply this equation to specific materials, it is necessary to obtain $\dot{\xi}$ as a function of the generalized displacements and their time derivatives. According to Eringen [14], if couple stresses and thermal effects are omitted,

$$\rho\dot{\xi} = \sigma_{ij}d_{ij} \tag{22}$$

where σ_{ij} is the stress tensor and d_{ij} is the deformation rate tensor. For the finite element representation, it is easily shown that

$$\sigma_{ij}d_{ij} = \sigma_{ij}c_{iN}(\delta_{kj} + c_{jM}u_{Mk})\dot{u}_{Nk} \tag{23}$$

We now assume that the material is homogeneous so that $\dot{\xi}$ is not a

function of the local coordinates x_i. In view of Eq. (22), it is a constant with respect to x_i for the finite element and can therefore be factored outside of the integral in Eq. (21). Noting also that

$$\rho_o = \sqrt{I_3}\,\rho \tag{24}$$

where I_3 is the third invariant in Eq. (12), and introducing Eqs. (22), (23), and (24) into Eq. (21), we arrive at the equation

$$\left[m_{NM}\ddot{u}_{Mi} + \sqrt{I_3}\,\sigma_{rs}c_{rN}(\delta_{is} + c_{sM}u_{Mi}) - p_{Ni}\right]\dot{u}_{Ni} = 0 \tag{25}$$

Since this equation must hold for all velocities $\dot{u}_{Ni}$, we have

$$m_{NM}\ddot{u}_{Mi} + \sqrt{I_3}\,\sigma_{rs}c_{rN}(\delta_{is} + c_{sM}u_{Mi}) = p_{Ni}(t) \tag{26}$$

It is now necessary to introduce into this equation the appropriate relation expressing the stress in terms of the strain, strain rates, higher-order strain rates, etc. in order to obtain the finite element representation for specific materials.

4. NONLINEAR STIFFNESS RELATIONS

We now examine applications of Eqs. (21) and (26) to various types of membranes.

4.1 Elastic Materials. In the case of elastic materials, the stress σ_{ij} is derivable from a potential function W which represents the strain energy per unit of undeformed volume. If each element is homogeneous, then ξ and W are not functions of the spatial coordinates x_i. It follows that

$$\int_V \rho_o \dot{\xi}\, dv_o = \int_V \dot{W}\, dv_o = v_o \dot{W} \tag{27}$$

where

$$\dot{W} = \frac{\partial W}{\partial u_{Ni}}\,\dot{u}_{Ni} \tag{28}$$

Introducing these equations into Eq. (21) and simplifying the results, we

obtain

$$(m_{NM}\ddot{u}_{Mi} + v_o \frac{\partial W}{\partial u_{Ni}} - p_{Ni})\dot{u}_{Ni} = 0 \tag{29}$$

This result must be valid for arbitrary node velocities of the element. Therefore

$$m_{NM}\ddot{u}_{Mi} + v_o \frac{\partial W}{\partial u_{Ni}} = p_{Ni} \tag{30}$$

Equation (30) is the general equation of motion for finite forced oscillations of an elastic membrane. For specific materials, the appropriate form of W must be introduced into this equation.

The important problem of small oscillations about a state of large deformation is obtained as a special case of Eq. (30) by denoting

$$u_{Ni} = \bar{u}_{Ni} + w_{Ni} \tag{31}$$

where $\bar{u}_{Ni}$ is the prescribed large displacement and w_{Ni} is a small perturbation. Then

$$m_{NM}\ddot{w}_{Mi} + f_u(\bar{u}_{Mi})w_{Mi} = \bar{p}_{Ni} \tag{32}$$

where

$$\bar{p}_{Ni} = p_{Ni} - v_o \frac{\partial W(\bar{u}_{Ni})}{\partial \bar{u}_{Ni}} \tag{33}$$

Here f_{NM} is known a known function of $\bar{u}_{Mi}$ and is independent of time. The forces $\bar{p}_{Ni}$ are known functions of time and Eq. (32) is linear in the dependent variables w_{Ni} and their derivatives.

If the membrane is in equilibrium, Eq. (30) reduces to [10,11]

$$p_{Ni} = v_o \frac{\partial W}{\partial u_{Ni}} \tag{34}$$

For elastic membranes, the stresses are calculated by means of the formulas

$$\sigma_{ij} = \frac{1}{2\sqrt{I_3}} \left(\frac{\partial W}{\partial \gamma_{ij}} + \frac{\partial W}{\partial \gamma_{ji}}\right) \tag{35}$$

4.1.1 Natural and Synthetic Rubbers. In the case of highly elastic materials such as natural and synthetic rubbers, several forms of the strain energy function W are available. Ordinarily, such materials are assumed to be incompressible and, for isotropic membranes, this incompressibility condition is equivalent to the condition

$$I_3 = 1 \tag{36}$$

Then, W is a function of only I_1 and I_2 and, instead of Eq. (35), the stresses are given by [13]

$$\begin{aligned} \sigma_{\alpha\beta} &= 2\delta_{\alpha\beta}\left(\frac{\partial W}{\partial I_1} + \lambda^2 \frac{\partial W}{\partial I_2}\right) + \left(\frac{2}{\lambda^2}\frac{\partial W}{\partial I_2} + p\right)g_{\alpha\beta} \\ \sigma_{\alpha 3} &= 0 \\ \sigma_{33} &= \lambda^2 \frac{\partial W}{\partial I_1} + \lambda^2(I_1 - \lambda^2)\frac{\partial W}{\partial I_2} + p \end{aligned} \tag{37}$$

where λ^2 is defined in Eq. (9), p is the hydrostatic pressure, and

$$g_{\alpha\beta} = \delta_{\alpha\beta} + 2\epsilon_{\mu\alpha}\epsilon_{\lambda\beta}\gamma_{\mu\lambda} \tag{38}$$

It is assumed that the membrane is very thin so that the strains are essentially uniform over the thickness and σ_{33}, the stress normal to the deformed surface, is negligible in comparison with $\sigma_{\alpha\beta}$. Then p can be determined from the condition $\sigma_{33} = 0$:

$$p = -\lambda^2 \frac{\partial W}{\partial I_1} - \lambda^2(I_1 - \lambda^2)\frac{\partial W}{\partial I_2} \tag{39}$$

Thus

$$\sigma_{\alpha\beta} = 2\delta_{\alpha\beta}\left(\frac{\partial W}{\partial I_1} + \lambda^2 \frac{\partial W}{\partial I_2}\right) + \left[\left(\lambda^4 + \frac{2}{\lambda^2} - \lambda^2 I_1\right)\frac{\partial W}{\partial I_2} - \lambda^2 \frac{\partial W}{\partial I_1}\right]g_{\alpha\beta} \tag{40}$$

Rivlin and Saunders [15,16] verified experimentally that the strain energy function for most isotropic, incompressible rubbers is of the form

$$W = C_1(I_1 - 3) + \Psi(I_2 - 3) \tag{41}$$

where C_1 is a material constant and the function Ψ depends upon the type of rubber. In analytical work, the most common form of W is the well-known

Mooney form [17]:

$$W = C_1(I_1 - 3) + C_2(I_2 - 3) \tag{42}$$

where C_1 and C_2 are experimentally determined constants. Treloar [18], using a statistical approach based on molecular theory, found for incompressible rubbers

$$W = C(I_1 - 3) \tag{43}$$

where C is a constant. Rivlin [19] refers to such materials as neo-Hookean.

To obtain nonlinear stiffness relations for finite elements of rubber membranes, first note that for incompressible membranes

$$\begin{aligned} I_1 &= \lambda^2 + 2(1 + \gamma_{\alpha\alpha}) \\ I_2 &= \frac{1}{\lambda^2} + 2\lambda^2(1 + \gamma_{\alpha\alpha}) \\ \lambda^2 &= (1 + 2\gamma_{\alpha\alpha} + \epsilon_{\alpha\beta}\epsilon_{\lambda\mu}\gamma_{\alpha\lambda}\gamma_{\beta\mu})^{-1} \end{aligned} \tag{44}$$

and

$$\begin{aligned} \frac{\partial\lambda^2}{\partial\gamma_{\alpha\beta}} &= -2\lambda^4 g_{\alpha\beta} \qquad \frac{\partial(1/\lambda^2)}{\partial\gamma_{\alpha\beta}} = 2g_{\alpha\beta} \\ \frac{\partial I_1}{\partial\gamma_{\alpha\beta}} &= 2(\delta_{\alpha\beta} - \lambda^4 g_{\alpha\beta}) \\ \frac{\partial I_2}{\partial\gamma_{\alpha\beta}} &= 2g_{\alpha\beta}(1 - 2\lambda^4 - 2\lambda^4\gamma_{\mu\mu}) + 2\lambda^2\delta_{\alpha\beta} \end{aligned} \tag{45}$$

where $g_{\alpha\beta}$ is defined in Eq. (38). For the finite element,

$$\begin{aligned} \lambda^2 = [1 + c_{\alpha N}(u_{N\alpha} + \frac{1}{2} c_{\alpha M}u_{Ni}u_{Mi}) + \epsilon_{\alpha\beta}\epsilon_{\lambda\mu}(c_{\alpha N}u_{N\lambda} \\ + \frac{1}{2} c_{\alpha N}c_{\lambda M}u_{Ni}u_{Mi})(c_{\beta L}u_{I\mu} + c_{\mu L}u_{L\beta} + c_{\beta K}c_{\mu L}u_{Kj}u_{Lk})]^{-1} \end{aligned} \tag{46}$$

and

$$g_{\alpha\beta} = \delta_{\alpha\beta} + \epsilon_{\mu\alpha}\epsilon_{\lambda\beta}(c_{\mu N}u_{N\lambda} + c_{\lambda N}u_{N\mu} + c_{\lambda M}c_{\mu N}u_{Ni}u_{Mi}) \tag{47}$$

wherein i, j, L, M, N, K = 1, 2, 3; α, β, λ, μ = 1, 2.

Introducing Eq. (42) and Eqs. (44)-(47) into Eqs. (34) and (40), we obtain the following equations for a finite element of a membrane of Mooney

material [11],

$$p_{Nk} = 2v_o c_{\alpha N}(\delta_{\beta j} + c_{\beta M}u_{Mk})\{C_1(\delta_{\alpha\beta} + \lambda^4 g_{\alpha\beta}) + C_2[g_{\alpha\beta}(1 - 2\lambda^4 - 2\lambda^4\gamma_{\mu\mu}) + \lambda^2\delta_{\alpha\beta}]\}$$

$$\sigma_{\alpha\beta} = 2\lambda\{C_1(\delta_{\alpha\beta} - \lambda^4 g_{\alpha\beta}) + C_2(\lambda^2\delta_{\alpha\beta} + (1 - 2\lambda^4 - 2\lambda^4\gamma_{\mu\mu})g_{\alpha\beta}\} \qquad (48a,b)$$

where

$$\gamma_{\mu\mu} = c_{\mu N}(u_{N\mu} + \frac{1}{2}c_{\mu M}u_{Ni}u_{Mi}) \qquad (49)$$

Similarly, for neo-Hookean membranes we find

$$p_{Nk} = 2v_o c_{\alpha N}C(\delta_{\alpha\beta} + c_{\beta M}u_{Mk})(\delta_{\alpha\beta} - \lambda^4 g_{\alpha\beta})$$

$$\sigma_{\alpha\beta} = 2\lambda\, C(\delta_{\alpha\beta} - \lambda^4 g_{\alpha\beta}) \qquad (50a,b)$$

Equations (48a) and (50a) are general nonlinear stiffness relations governing the static behavior of finite elements of Mooney and neo-Hookean membranes. Upon connecting the elements appropriately and applying boundary conditions, these lead to systems of nonlinear algebraic equations in the node displacements. Once solved, the results are introduced into Eqs. (10), (48b), and (50b) to obtain final strains and stresses in the structure.

4.1.2 Plastics and Nonlinearly Elastic Materials. Recent experiments on plastics and synthetic materials have attempted to arrive at approximate energy functions for such materials even through their behavior is not always perfectly elastic. These have led to highly nonlinear forms for the potential function W. For example, experiments on a dimethyl siloxane rubber by Hutchinson, Becker, and Landel [20] have indicated an energy function of the form

$$W = B_1(I_1 - 3) + B_2(I_1 - 3)^2 + B_3\{1 - \exp[b_1(I_2 - 3)]\} + B_4\{1 - \exp[b_2(I_2 - 3)]\} \qquad (51)$$

where B_1, B_2, B_3, B_4, b_1, and b_2 are material constants.

In this case, the nonlinear stiffness relation is given by

$$p_{Nk} = 2v_o c_{\alpha N}(\delta_{\alpha\beta} + c_{\beta M}u_{Mk})\{[B_1 + 2B_2(I_1 - 3)](\delta_{\alpha\beta} - \lambda^4 g_{\alpha\beta}) - (I - 3)\{B_3 b_1 \exp[b_1(I_3 - 3)] + B_4 b_2 \exp[b_2(I_2 - 3)]\}[g_{\alpha\beta}(1 - 2\lambda^4 - 2\lambda^4\gamma_{\mu\mu}) + \lambda^2\delta_{\alpha\beta}]\} \quad (52)$$

as before, stresses are computed by means of Eq. (40).

4.1.3 Metals and Reinforced Fabrics. Deformations of metallic and reinforced fabric pneumatic structures are usually characterized by large displacements accompanied by strains which are small in comparison with unity. In such cases, the material is assumed to be homogeneous and elastic within each finite element and the well-known Hookean form of the strain energy function is applicable. Moreover, the strain normal to the deformed surface can then be expressed as a linear function of the strains in the middle surface and the state-of-strain is described by the two-dimensional tensor $\gamma_{\alpha\beta}$. The strain energy function is therefore of the form

$$W = \frac{1}{2}E_{\alpha\beta\lambda\mu}\gamma_{\alpha\beta}\gamma_{\lambda\mu} \quad (53)$$

where $E_{\alpha\beta\lambda\mu}$ is a multi-dimensional array of elastic constants. The stress tensor is given by

$$\sigma_{\alpha\beta} = E_{\alpha\beta\lambda\mu}\gamma_{\lambda\mu} = E_{\alpha\beta\lambda\mu}c_{\lambda N}(u_{N\mu} + \frac{1}{2}c_{\mu M}u_{Mi}u_{Ni}) \quad (54a)$$

and the nonlinear stiffness relation for the finite element is obtained by introducing Eq. (53) into Eq. (34):

$$p_{Nk} = v_o c_{\alpha N}(\delta_{\beta M} + c_{\beta M}u_{Mk})E_{\alpha\beta\lambda\mu}c_{\lambda I}(\delta_{\mu i} + \frac{1}{2}c_{\mu J}u_{Ji})u_{Ii}$$

$$I,J,M,N,i,k, = 1,2,3; \quad \alpha,\beta,\lambda,\mu = 1,2 \quad (54b)$$

The array of material constants, $E_{\alpha\beta\lambda\mu}$, possess the symmetric properties

$$E_{\alpha\beta\lambda\mu} = E_{\beta\alpha\lambda\mu} = E_{\alpha\beta\mu\lambda} = E_{\lambda\mu\alpha\beta} \quad (55)$$

and, for isotropic materials, it is given by

$$E_{\alpha\beta\lambda\mu} = \frac{E}{2(1+\nu)} \left(\delta_{\alpha\beta}\delta_{\beta\lambda} + \delta_{\alpha\lambda}\delta_{\beta\mu} + \frac{2\nu}{1-\nu}\,\delta_{\alpha\beta}\delta_{\lambda\mu}\right) \tag{56}$$

where E is Young's modulus and ν is Poisson's ratio.

The form of $E_{\alpha\beta\lambda\mu}$ in Eq. (56) is applicable to most engineering metals (steel, aluminum, and tungsten, etc.) and to isotropic fabrics. However, most of the reinforced fabric and composite materials are either completely anisotropic or transversely isotropic only with respect to a normal to the middle surface.

A typical example of such a reinforced fabric is indicated in Fig. 3. Here a fabric core material, which is assumed to be isotropic and to have a modulus E and Poisson's rate ν, is reinforced by a network of fibers of modulus $\overline{E}$ and Poisson's ratio $\overline{\nu}$. The fibers form an angle α with respect to the y_1-axis, as shown. When the fiber spacing is relatively small, it is convenient to introduce mean values for the appropriate material constants of the composite structure. Thus, we introduce the following constants [21]:

$$\begin{aligned} E_1 &= k\overline{E} + (1-k)E \\ E_2 &= \frac{E\overline{E}}{kE + (1-1)\overline{E}} \\ G_c &= \frac{G\overline{G}}{kG + (1-k)\overline{G}} \\ \nu_c &= k\overline{\nu} + (1-k)\nu \end{aligned} \tag{57}$$

where k is the ratio of the cross-sectional area of the fibers to the total cross-sectional area of the element, G and $\overline{G}$ are the respective shear moduli of the core fabric and the fibers, E_1 and E_2 are respectively the effective mean moduli of elasticity in the y_1 and y_2 directions, G_c is the mean shear modulus, and ν_c is the mean Poisson's ratio of the composite material. We

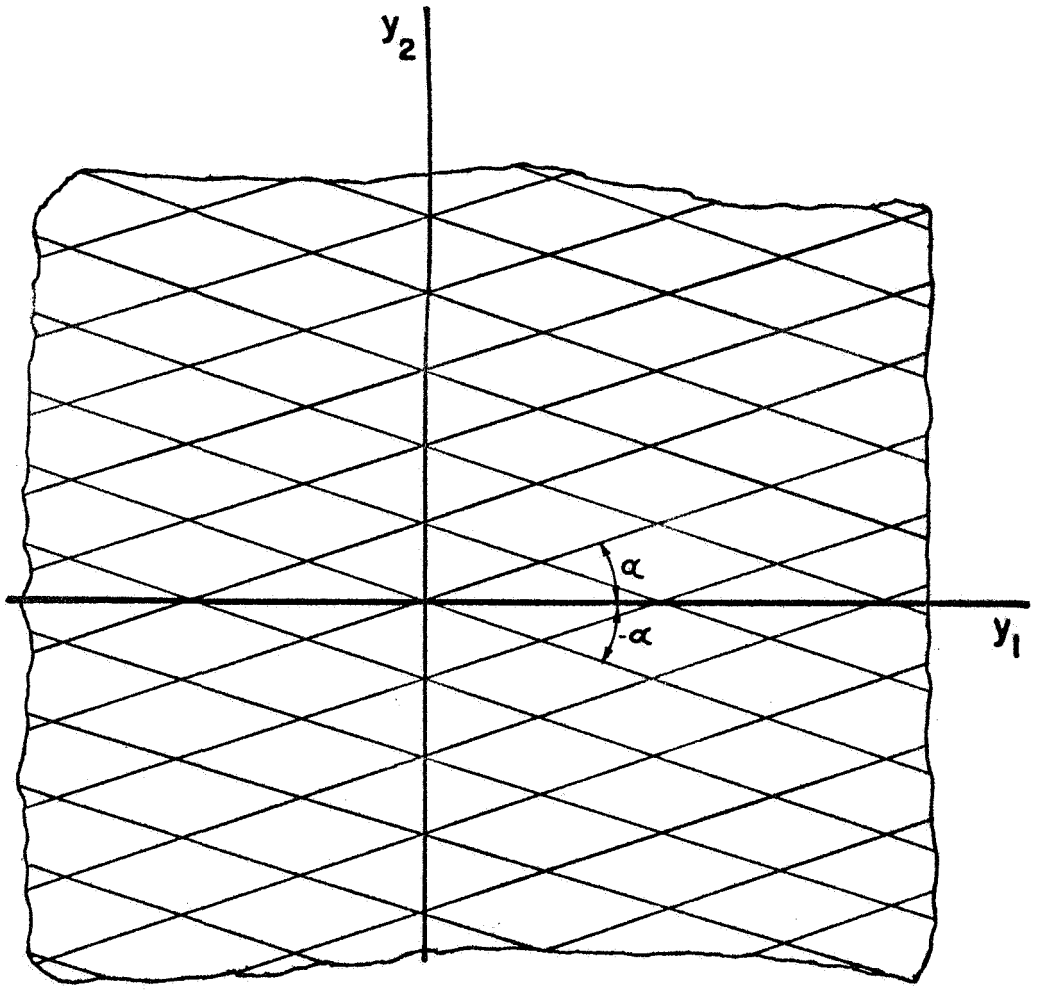

FIG. 3 Fiber reinforcement pattern in composite fabric sheet.

then have

$$
\begin{aligned}
E_{1111} &= a_{11}\cos^4\alpha + a_{22}\sin^4\alpha + 2(a_{12} + 2G_c)\sin^2\alpha\cos^2\alpha \\
E_{1122} &= E_{2211} = (a_{11} + a_{22} - 4G_c)\sin^2\alpha\cos^2\alpha + a_{12}(\sin^4\alpha + \cos^4\alpha) \\
E_{2222} &= a_{11}\sin^4\alpha + a_{22}\cos^4\alpha + 2(a_{12} + 2G_c)\sin^2\alpha\cos^2\alpha \\
E_{1212} &= E_{1221} = E_{2112} = E_{2121} = (a_{11} + a_{22} - 2a_{12})\sin^2\alpha\cos^2\alpha \\
&\qquad + G_c(\cos^2\alpha - \sin^2\alpha)^2 \\
E_{1112} &= E_{1121} = E_{2212} = E_{2221} = E_{1211} = E_{1222} = E_{2122} = 0
\end{aligned}
\tag{58}
$$

where

$$
\begin{aligned}
a_{11} &= \frac{E_2}{1 - \nu_c^2 E_1/E_2} \\
a_{22} &= \frac{E_1}{1 - \nu_c^2 E_1/E_2} \\
a_{12} &= a_{21} = \frac{\nu_c E_1}{1 - \nu_c^2 E_1/E_2}
\end{aligned}
\tag{59}
$$

4.2 Viscoelastic Materials. The equations of motion of a finite element of a viscoelastic material are obtained by introducing the appropriate constitutive equation, written explicitly in terms of the stress tensor σ_{ij}, into Eq. (26). We confine our attention to isotropic materials for which the stress is dependent on the displacement and velocity gradients. In general, the constitutive equations for such materials can be written in the form

$$
\sigma_{ij} = \mathcal{F}\left(\frac{\partial y_r}{\partial x_r}, \frac{\partial \dot{u}_r}{\partial y_r}\right)_{\tau=-\infty}^{\tau=t} \tag{60}
$$

where $\mathcal{F}$ is a tensor functional of the indicated arguments. Then the equations of motion for a finite element are

$$
m_{NM}\ddot{u}_{Mi} + \sqrt{I_3}\,\mathcal{F}\left(\frac{\partial y_r}{\partial x_r}, \frac{\partial u_r}{\partial y_r}\right)_{\tau=-\infty}^{\tau=t} c_{rN}(\delta_{is} + c_{sM}u_{Mi}) = p_{Ni}(t) \tag{61}
$$

Specific forms of these relations for given materials are obtained by introducing the appropriate expanded form of $\mathcal{I}$ in Eq. (61).

Although a detailed discussion of finite element formulations for nonlinearly viscoelastic materials is outside the scope of the present investigation, the general procedure is amply demonstrated by a simple example. Consider the case of plane stress in a thin membrane undergoing large displacements but strains which are small in comparison with unity, and, for simplicity, assume that the membrane is constructed of a simple linearly viscoelastic material of Voigt type:

$$\sigma_{\alpha\beta} = A_{\alpha\beta\lambda\mu}\gamma_{\lambda\mu} + B_{\alpha\beta\lambda\mu}d_{\lambda\mu} \tag{62}$$

Here $A_{\alpha\beta\lambda\mu}$ and $B_{\alpha\beta\lambda\mu}$ are arrays of material parameters and may be functions of time. Then Eq. (26) becomes

$$m_{NM}\ddot{u}_{Mi} + c_{\alpha N}c_{\lambda I}(\delta_{i\beta} + c_{\beta M}u_{Mi})[A_{\alpha\beta\lambda\mu}(\delta_{\mu m} + \tfrac{1}{2}c_{\mu J}u_{Jm})u_{Im} + B_{\alpha\beta\lambda\mu}(\delta_{\mu m} + c_{\mu J}u_{Jm})\dot{u}_{Im}] = p^{(t)}_{Ni} \tag{63}$$

We obtain a system of linear differential equations describing the in-plane motion of flat viscoelastic elements by deleting products and squares of the displacements and velocities in Eq. (63) and limiting the ranges of lower-case indices to 2:

$$m_{NM}\ddot{u}_{M\alpha} + B_{\beta\alpha\lambda\mu}c_{\beta N}c_{\lambda M}c_{M\mu} + A_{\beta\alpha\lambda\mu}c_{\beta N}c_{\lambda M}u_{M\mu} = p^{(t)}_{N\alpha} \tag{64}$$

It is seen that the above procedure provides a systematic and rational means for identifying the material damping coefficients for any material for which the stress is given explicitly as a function of strains, strain rates, and other kinematic variables.

4.3 Elasto-plastic Materials. It is not difficult to modify finite element

formulations so as to account for yielding and plastic deformation of metallic membranes. Since, in view of Eqs. (10), the strain components are uniform throughout each triangular element, so also in the stress [Eq. (54)]. Thus, if local yielding is imminent, it is characterized by uniform yielding and strain hardening of the associated local finite elements. This means that elastic-plastic boundaries cannot move continuously during an incremental loading process; but this characteristic of the discrete model need not lead to divergent or inconsistent results.

In this investigation, the approach suggested by Pope [22,23] is extended so as to apply to large displacements of elasto-plastic membranes. The elasto-plastic behavior of a typical finite element is analyzed through an incremental loading process. During each increment, the material responds linearly, but the overall response obtained by summing the incremental values may be highly nonlinear.

Let $\sigma^o_{\alpha\beta}$, $\gamma^o_{\alpha\beta}$, p^o_{Ni}, and u^o_{Ni} denote the known values of the stress, strain, node forces, and node displacements at some reference state o in a typical finite element and let $\delta\sigma_{\alpha\beta}$, $\delta\gamma_{\alpha\beta}$, δp_{Ni}, and δu_{Ni} denote small increments in these quantities. If these increments are sufficiently small, it can be easily shown that

$$\delta\gamma_{\alpha\beta} = \gamma_{\alpha\beta} - \gamma^o_{\alpha\beta} = \delta\gamma^e_{\alpha\beta} + \delta\gamma^p_{\alpha\beta}$$

$$\delta\gamma^e_{\alpha\beta} + \delta\gamma^p_{\alpha\beta} = c_{\alpha N}(\delta_{\beta i} + c_{\beta M} u^o_{Mi})\delta u_{Ni} \qquad (65a,b,c)$$

$$\delta p_{Ni} = c_{\alpha N}(\delta_{\beta i} + c_{\beta M} u^o_{Mi})\delta\sigma_{\alpha\beta} + c_{\alpha N} c_{\beta M} \sigma^o_{\alpha\beta} \delta u_{Mi}$$

where $\delta\gamma^e_{\alpha\beta}$ is the elastic strain increment and $\delta\gamma^p_{\alpha\beta}$ is the plastic strain increment. The term $(\delta_{\beta i} + c_{\beta M} u^o_{Mi})$ in Eq. (65c) represents the influence of large displacements on the relationship between stresses and the node forces.

The term $c_{\beta M}u^{o}_{Mi}$ an be neglected in the case of small displacements.

The elastic strain increment is related to the stress increment according to

$$\delta\sigma_{\alpha\beta} = \sigma_{\alpha\beta} - \sigma^{o}_{\alpha\beta} = E^{o}_{\alpha\beta\lambda\mu}\delta\gamma^{e}_{\lambda\mu} \tag{66}$$

in which the array $E^{o}_{\alpha\beta\lambda\mu}$ may, in general, be a function of $\gamma^{o}_{\alpha\beta}$.

The yield condition may be represented by a convex yield surface in stress space which is given by [24]

$$f(\sigma_{ij}) = 0 \tag{67}$$

The yield function f is symmetrical with respect to σ_{ij} and σ_{ji} and depends upon the strain history of the membrane. Since it is assumed that plastic deformation is independent of the hydrostatic stress, we can rewrite (67) in the form

$$f(\overline{\sigma}_{ij}) = 0 \tag{68}$$

where $\overline{\sigma}_{ij}$ is the stress deviator:

$$\overline{\sigma}_{ij} = \sigma_{ij} - \frac{1}{3}\delta_{ij}\sigma_{kk} \tag{69}$$

When the stress increment $\delta\sigma_{\alpha\beta}(\sigma_{3\alpha} = \sigma_{33} = 0)$ does not have a positive component in the direction of an inward normal to the yield surface and when the stress point $\sigma_{\alpha\beta}$ lies on the yield surface, the material yields and the plastic strain increment is given by

$$\delta\gamma^{p}_{\alpha\beta} = \mu\frac{\partial f}{\partial\sigma_{\alpha\beta}} \tag{70}$$

The factor μ depends upon the strain history and is independent of all components of $\delta\sigma_{\alpha\beta}$ except that normal to the field surface.

At initial yielding, the yield condition (68) is satisfied. After an additional increment of plastic strain, the yield condition is given by

$$f + t_{\alpha\beta}\delta\gamma^{p}_{\alpha\beta} + \frac{\partial f}{\partial\sigma_{\alpha\beta}}\delta\sigma_{\alpha\beta} = 0 \tag{71}$$

where $t_{\alpha\beta}$ describes the strain-hardening properties of the material. Introducing Eqs. (66), (68), and (70) into (71) and simplifying the results, we find that

$$\mu = \frac{\frac{\partial f}{\partial \sigma_{\alpha\beta}} \delta\sigma_{\alpha\beta}}{E^{o}_{\alpha\beta\lambda\mu} \frac{\partial f}{\partial \sigma_{\alpha\beta}} \frac{\partial f}{\partial \sigma_{\lambda\mu}} - t_{\alpha\beta} \frac{\partial f}{\partial \sigma_{\alpha\beta}}} \tag{72}$$

Thus

$$\delta\gamma^{p}_{\alpha\beta} = G_{\alpha\beta\lambda\mu}\delta\sigma_{\lambda\mu} \tag{73}$$

where

$$G_{\alpha\beta\lambda\mu} = \frac{\frac{\partial f}{\partial \sigma_{\alpha\beta}} \frac{\partial f}{\partial \sigma_{\lambda\mu}}}{E^{o}_{\xi\eta\delta\rho} \frac{\partial f}{\partial \sigma_{\xi\eta}} \frac{\partial f}{\partial \sigma_{\delta\rho}} - t_{\xi\eta} \frac{\partial f}{\partial \sigma_{\xi\eta}}} \tag{74}$$

Introducing Eqs. (73) and (66) into (65b) and solving for $\delta\sigma_{\alpha\beta}$, we obtain

$$\delta\sigma_{\alpha\beta} = H^{o}_{\alpha\beta\lambda\mu} c_{\lambda N}(\delta_{\mu j} + c_{\mu M} u^{o}_{Mj})\delta u_{Nj} \tag{75}$$

where $H^{o}_{\alpha\beta\lambda\mu}$ is the inverse of $G^{o}_{\alpha\beta\lambda\mu} + E^{o}_{\alpha\beta\lambda\mu}$:

$$H^{o}_{\alpha\beta\lambda\mu}(G_{\lambda\mu\rho\nu} + E^{o}_{\lambda\mu\rho\nu})^{-1} = \delta_{\alpha\rho}\delta_{\lambda\mu} \tag{76}$$

Finally, Eq. (65c) becomes

$$\delta p_{Ni} = [c_{\alpha N}(\delta_{\beta i} + c_{\beta M} u^{o}_{Mi}) H^{o}_{\alpha\beta\lambda\mu} c_{\lambda R}(\delta_{\mu j} + c_{\mu M} u^{o}_{Mj}) + \delta_{ij} c_{\alpha N} c_{\beta R} \sigma^{o}_{\alpha\beta}]\delta u_{Rj} \tag{77}$$

Equation (77) represents the stiffness relation between the incremental loads δp_{Ni} and their cooresponding incremental displacements. These equations are inverted for each load increment; the solutions δu_{Ni} are introduced into Eq. (75) to obtain the associated stress increment. Incremental strains $\delta\gamma^{e}_{\alpha\beta}$ and $\delta\gamma^{p}_{\alpha\beta}$ are then calculated by means of Eqs. (66) and (73). Once the

incremental values δu_{Ni}, $\delta\sigma_{\alpha\beta}$, and $\delta\gamma_{\alpha\beta}$ are determined, they are added algebraically to those of the reference state (i.e., u^o_{Ni}, $\sigma^o_{\alpha\beta}$, $\gamma^o_{\alpha\beta}$) to obtain a new reference state ($u^{o'}_{Ni} = u^o_{Ni} + \delta u_{Ni}$, $\sigma^{o'}_{\alpha\beta} = \sigma^{o'}_{\alpha\beta} + \delta\sigma_{\alpha\beta}$, etc.) and the process is repeated for a new load increment. Following the procedure indicated by Pope [22], during each cycle the factor μ of each element is examined. If $\mu < 0$, the element is added to the elastic region of the membrane and the analysis is repeated; if the mean stress over a load increment is on or outside the yield surface, the analysis is repeated with the element permitted to deform plastically. Accuracy is improved by choosing the load increments such that one element, at the most, yields during each load increment. Other details of the procedure are identical to those of the small displacement case and can be found in references [22] and [23].

5. FORMULATION OF THE STRUCTURAL PROBLEM

5.1 Global Equations of Motion. The nonlinear equations derived in the previous section describe the behavior of a single finite membrane within its local reference frame; these relations are independent of the loading on the membrane, the boundary conditions, or the location of the element in the assembled system. It is now necessary to connect the elements at appropriate node points and to sum their properties so as to represent a pneumatic structure of specified shape with specified boundary conditions. To accomplish this, it is convenient to first rotate the node forces, displacements, velocities, accelerations, and local coordinates associated with each element so that they are parallel to the global reference frame Z_i. This is accomplished through the transformations

$$\begin{aligned}
\bar{p}_{Mie} &= \beta_{kie}\underline{p}_{Mke} \\
u_{Mke} &= \beta_{kie}\underline{\bar{u}}_{Mie} \\
\dot{u}_{Mke} &= \beta_{kie}\underline{\dot{\bar{u}}}_{Mie} \\
\ddot{u}_{Mke} &= \beta_{kie}\underline{\dot{u}}_{Mie} \\
x_{ie} &= \beta_{kie}\underline{x}_{ke}
\end{aligned} \tag{78}$$

where the underscore (e) indicates that no sum is to be taken on the repeated index e. In these equations, $\bar{p}_{Mie}$, $\bar{u}_{Mie}$, $\dot{\bar{u}}_{Mie}$, and $\ddot{\bar{u}}_{Mie}$ are respectively, the node forces, displacements, velocities, and accelerations of node M of element e in the direction of Z_i, $\bar{x}_{ie}$ are the rotated local coordinates defined in Eq. (1), and β_{kie} is the cosine of the angle between $\bar{x}_{ie}$ and x_{ke}. The ranges of the indices in these equations are M, i, k, = 1, 2, 3 and e = 1, 2, ..., E_e where E_e is the total number of finite elements.

It was pointed out earlier that the set of numbers Z_{Ni}(i = 1,2,3; N = 1,2, ..., n) describes the geometry of the assembled (connected) system whereas $\bar{x}_{Nie}$(N, i = 1,2,3; e = 1,2, ..., E_e) decribes that of the individual elements. The connectivity of the system is established by relating the members of the set Z_{Ni} to those of $\bar{x}_{Nie}$ by the transformation

$$\bar{x}_{Mie} = \Omega_{Mie} Z_{Ni} \quad (M = 1, 2, 3;\ N = 1, 2, \ldots, n) \tag{79}$$

where

$$\Omega_{MNe} = \begin{cases} 1 & \text{if node M of element e is identical to node N in the assembled system} \\ 0 & \text{if otherwise} \end{cases} \tag{80}$$

The transformation indicated in Eq. (79) defines a mapping of points in the set Z_{Ni} into points in $\bar{x}_{Mie}$ and, in effect, assembles the elements into a single unit. The process is illustrated symbolically for the case $E_e = 4$, n = 5 in Fig. 4.

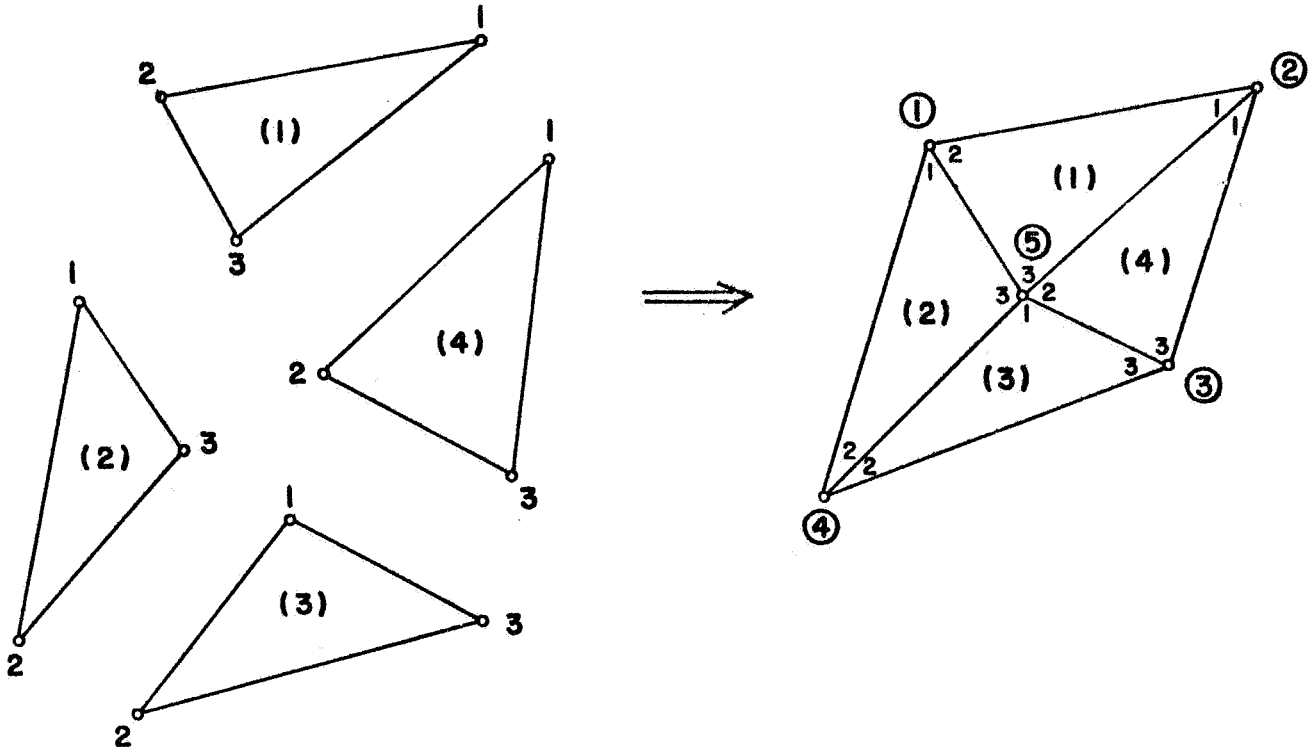

LOCAL SYSTEMS

$\bar{x}_{Mie}$

e = 1,2,3,4 (ELEMENT INDEX)

M = 1,2,3 (LOCAL NODE INDEX)

i = 1,2,3 (COORDINATE INDEX)

GLOBAL SYSTEM

Z_{Ni}

N = 1,2,3,4,5 (GLOBAL NODE INDEX)

i = 1,2,3 (COORDINATE INDEX)

$$\bar{x}_{Mie} = \Omega_{MNe} Z_{Mi}$$

FIG. 4 Assembly of elements through transformations of points in global set Z_{Ni} into local sets $\bar{x}_{Mie}$.

Similarly, if P_{Nk}, U_{Nk}, $\dot{U}_{Nk}$, and $\ddot{U}_{Nk}$ denote the values of node forces, displacements, velocities,and accelerations in the assembled system, it can be shown that

$$\begin{aligned} P_{Nk} &= \Omega_{MNe}\bar{p}_{Mke} \\ \bar{u}_{Mke} &= \Omega_{MNe}U_{Nk} \\ \dot{\bar{u}}_{Mke} &= \Omega_{MNe}\dot{U}_{Nk} \\ \ddot{\bar{u}}_{Mke} &= \Omega_{MNe}\ddot{U}_{Nk} \end{aligned} \tag{81}$$

In this case, the repeated indices N and e are summed throughout their entire ranges: N= 1, 2, ..., n; e = 1, 2, ..., E_e.

Application of Eqs. (78) through (81) assembles the finite elements into a single discrete system. When the local variables appearing in local equations of motion [such as Eqs. (21) or (26)] are transformed in accordance with Eqs. (78) and (81), the resulting relation is referred to as a global equation of motion. In particular, Eq. (21) becomes

$$P_{Ni}\dot{U}_{Ni} = M_{NM}\ddot{U}_{Mi}\dot{U}_{Ni} + \int_{V_o}\rho_o\dot{\xi}dV_o \tag{82}$$

where

$$M_{NM} = \sum_{e=1}^{E_e}\Omega_{RMe}\Omega_{SNe}m_{RSe} \tag{83}$$

In this case N, M = 1, 2 ..., n; R, S = 1, 2, 3 and the integration is carried out over the entire volume V_o of the undeformed structure. Equation (82) is the general global equation of motion of a finite element.

Global equations for the case of static behavior are of special interest. In this case,the local equations of motion reduce to nonlinear stiffness relations of the form

$$p_{Mme} = k(u_{Nke}) \tag{84}$$

where $k(u_{Nke})$ is the appropriate nonlinear function of the node displacements. For example, the function $k(u_{Nke})$ for synthetic rubbers, nonlinearly elastic materials, and Hookean metals are defined by Eqs. (48a), (52), and (54) respectively. When the components of node forces and displacements are rotated so that they are parallel to the coordinates $\bar{x}_{ie}$, Eq. (84) becomes

$$\bar{p}_{Mie} = \beta_{ime} k(\beta_{kje} \bar{u}_{Nje}) \tag{85}$$

Finally, the global stiffness relations are obtained through the transformations indicated in Eq. (81):

$$P_{Nk} = \mathcal{K}_{Nk}(U_{Rs}) \tag{86}$$

where

$$\mathcal{K}_{Nk}(U_{Rs}) = \Omega_{MNe} \beta_{ike} k(\beta_{kje} \Omega_{SRe} U_{Rs}) \tag{87}$$

Boundary conditions are applied by prescribing generalized (global) displacements at appropriate boundary nodes. Then Eqs. (86) reduce to a system of independent nonlinear algebraic equations in the unknown node displacements.

5.2 External Pressure. Up to this point, the relations derived are applicable only to situations in which the loads do not change in direction as the structure deforms. Since, for pneumatic structures, this is obviously a severe restriction, a procedure [7,11] for accounting for changes in the external loading due to deformation is now examined.

It is first assumed that the dimensions of each finite element are sufficiently small that the pressure q can be regarded as uniform over the surfaces of each finite element. Then, if A denotes the area of the deformed element, the total force exerted normal to the plane of the element is

$$\tilde{q} = Aq \tag{88}$$

Let n_i denote the components of an outward unit vector normal to A. Then the components of the pressure force $\tilde{q}$ are given by

$$\tilde{q}_i = n_i A q \tag{89}$$

To determine the components n_i, the coordinates of nodes of the deformed element are denoted

$$y_{Ni} = x_{Ni} + u_{Ni} \tag{90}$$

For convenience in writing, the origin of the reference frame y_i is transferred to node 3 of the deformed element. If the resulting coordinate system is denoted z_i, it follows that

$$z_{Ni} = y_{Ni} - y_{3i} \tag{91}$$

Now consider two unit vectors emanating from the origin of the coordinates z_i (node 3). The components n_i of the unit normal are obtained by forming the vector product of these two vectors:

$$n_i = \frac{1}{2A} \epsilon_{ijk} z_{1j} z_{2k} \tag{92}$$

where ϵ_{ijk} is the permutation symbol. Thus, equation (89) can be written

$$q_i = \frac{1}{2} q \epsilon_{ijk} z_{1j} z_{2k} \tag{93}$$

The net external force at each node is obtained by simply representing q by three forces, one at each node, whose components are

$$Q_i = \frac{1}{6} q \epsilon_{ijk} z_{1j} z_{2k} \tag{94}$$

Introducing Eq. (91) gives

$$Q_i = \frac{1}{6} q \epsilon_{ijk} (y_{1j} y_{2k} + y_{2j} u_{3k} + y_{3j} y_{1k}) \tag{95}$$

This result defines the generalized external force in the deformed element produced by external pressure. Note that no node identification index is needed since Q_i is the same for each node of the element.

To complete the analysis, these forces are now transformed into components $\bar{Q}_i$ parallel to the local reference frame $\bar{x}_i$. The result for element e is

$$\bar{Q}_{ie} = \frac{1}{12} q_e \sum_{p=1}^{3} \epsilon_{pMN} \epsilon_{ijk} (\bar{x}_{Nj\underline{e}} + \bar{u}_{Nj\underline{e}})(\bar{x}_{Mk\underline{e}} + \bar{u}_{Mk\underline{e}}) \tag{96}$$

wherein the underscore again indicates that no sum is to be taken on the repeated index e.

In the case of pressure loadings, the component $\bar{Q}_{ie}$ take the place of the node forces $\bar{p}_{Nie}$ of Eqs. (78) and (85). It is seldom necessary to transform these components into the global system, however, since it is more convenient to first transform displacements into the $\bar{x}_i$ system with the aid of Eq. (1) and then to transform the resulting forces into the global system.

5.3 Solution of Nonlinear Equations. In the case of time-dependent phenomena, finite element formulations lead to systems of simultaneous nonlinear differential equations of the form indicated in Eqs. (26), (63), and (82). The solution of such systems of equations is a formidable task, even with the aid of modern digital computers. Generalizations of the well-known Runga-Kutta techniques may lead to acceptable results in some cases; but general procedures for solving such large systems of coupled nonlinear differential equations are, at best, still in the early stages of development. It is important to note, however, that numerical procedures are available for the solution of nonlinear algebraic equations; and by incrementing the time variable t, the original set of differential equations reduce to a system of nonlinear algebraic equations for each time increment. Moreover, finite element representations of static behavior in pneumatic structures also lead to systems of nonlinear algebraic equations. In view of this, the solution of large systems of nonlinear differential equations is not considered further

in this study. Rather, consideration is given to procedures for solving systems of nonlinear algebraic equations, it being understood that, at the cost of greatly increasing the computing time, these procedures can also be applied to certain systems of nonlinear differential equations.

Several numerical schemes for solving simultaneous nonlinear algebraic equations are available in the literature; but not all of these are suitable for systems of equations as large as those encountered in the present investigation. A comprehensive review and comparison of numerical procedures for equations of this type was recently contributed by Remmler, Cawood, Stanton, and Hill [25], wherein numerical experimentation showed that the classical Newton-Raphson method and the Fletcher-Powell method are among the most efficient and reliable techniques available. To these may be added the method of incremental loading, which is somewhat related to the Newton-Raphson method, except that the loading is assumed to be applied small increments during each of which the structure responds linearly. This latter technique is particularly well-suited for the analysis of stability and plastic behavior. The numerical results to be presented subsequently were obtained using variations of the Newton-Raphson method. Thus, for the present discussion, it sufficies to merely outline this procedure. Details of this and other numerical procedures can be found in the report by Remmler et al [25] and in the papers by Sprang [26] and Brooks [27].

Consider a system of nonlinear stiffness relations of the form in Eq. (86). Assuming that after appropriate boundary conditions have been applied there remain r unprescribed components of node displacements, this system represents a set of r independent nonlinear equations in the unknown displacements U_{Nk}. For simplicity, suppose that these equations are represented in matrix form as

$$\mathbf{H}(\mathbf{U}) = \mathbf{O} \tag{97}$$

where $\mathbf{H}$ is a r x 1 column matrix, each row of which represents an independent nonlinear stiffness equation, and $\mathbf{U}$ is the solution vector. To solve these equations, we expand $\mathbf{H}$ in a Taylor series about an arbitrary point $\mathbf{U}^{\circ}$ which represents an initial estimate of the solution $\mathbf{U}$. The vector $\mathbf{U}^{\circ}$ may, for example, correspond to the linearized solution. Taking only two terms, we find

$$\mathbf{H}(\mathbf{U}) = \mathbf{H}(\mathbf{U}^{\circ}) + \mathbf{J}(\mathbf{H}^{\circ})(\mathbf{U} - \mathbf{U}^{\circ}) \tag{98}$$

where is the jacobian matrix

$$\mathbf{J} = \left[\frac{\partial H_i}{\partial U_j}\right] \tag{99}$$

Equation (98) is linear in $\mathbf{U}$. Solving this equation, we find

$$\mathbf{U} = \mathbf{U}^{\circ} - \mathbf{J}(\mathbf{U}^{\circ})^{-1}\mathbf{H}(\mathbf{U}^{\circ}) \tag{100}$$

The corrected solution $\mathbf{U}$ serves as the initial estimate in a second cycle, and the process is continued until a desired degree of accuracy is obtained.

6. NUMERICAL AND EXPERIMENTAL RESULTS

In this section, we examine numerical results obtained by applying the theory developed in the preceding sections to several representative problems. Whenever possible, these results are compared with available experimental or analytical data.

6.1 Stress Diffussion in a Stiffened Panel. Ordinarily, stresses obtained from finite element analyses based on approximate displacement fields are less accurate than displacements obtained from such models. To get an indication of the accuracy of stresses derived from a rather coarse finite element representation, and also to examine an elementary problem involving

composite bar and plate elements, the problem of plane stress in a reinforced panel was considered as a simple first example. In this case, deformations are assumed to be small and elastic and the material is assumed to be homogeneous and isotropic. Equations (54) and (56) are applicable except that only in-plane deformations are considered and products and squares of displacements are neglected in comparison with the displacements themselves.

The stiffened panel shown in Fig. 5a was analyzed using the finite element representation in Fig. 5b. Here a rectangular panel 0.127 mm. thick, stiffened by longitudinal rods of area 1.613 cm^2 on the outside and 0.807 cm^2 along the centerline, is subjected to concentrated forces of 1,587 kg, as is indicated. An elastic modulus of 703,000 kg/cm^2 and a Poisson's ratio of 0.3 were used. The computed variation of the normal stress in the exterior longitudinal stiffeners with the distance x from the fixed edge is shown in Fig. 5c compared with results obtained from an approximate theory developed by Kuhn [28]. We observe that the coarse finite-element representation yielded stresses, in this case, which are in close agreement with those predicted by Kuhn's theory.

6.2 Elasto-plastic Behavior of a Metallic Membrane. The finite element formulation described in Section 4.3 was used in the analysis of plastic behavior of a square aluminum membrane subjected to external pressure. A bilinear stress-strain law of the form indicated in Fig. 6 was assumed with $\sigma_y = 2{,}514$ kg/cm^2, $\gamma_y = 0.0034$, $E_e = 20E_p = 740{,}000$ kg/cm^2. These properties correspond to the aluminum alloy 2014-73 and agree closely with those used in experiments on rectangular shell plating by Neubert and Sommer [29]. A thin metallic sheet, 60 cm. square and 0.14 cm. thick, is subjected to a uniformly distributed hydrostatic pressure. As the pressure is slowly increased, a region near the center of the plate yields and plastic flow is initiated.

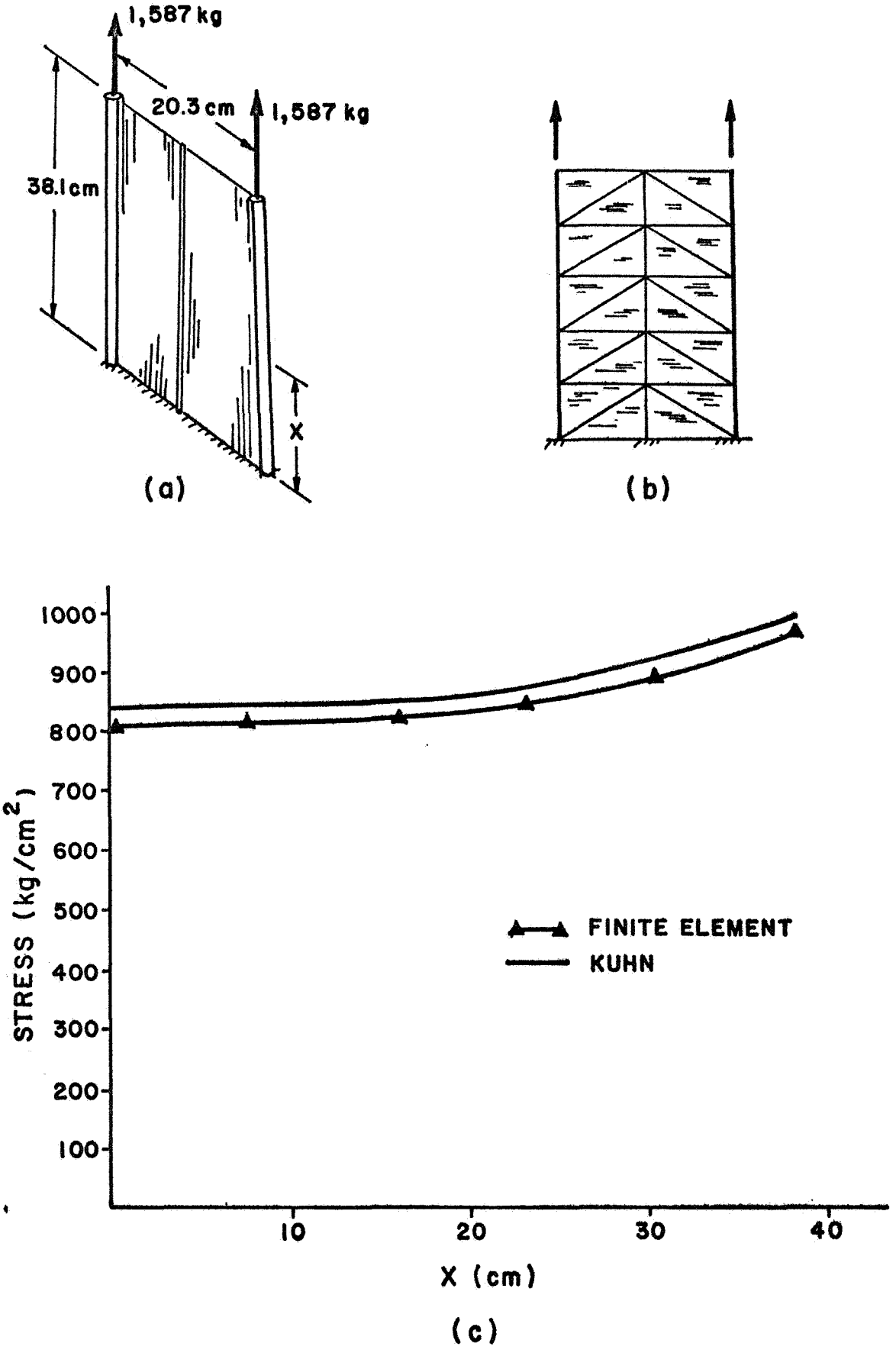

FIG. 5 Plane stress in a stiffened panel.

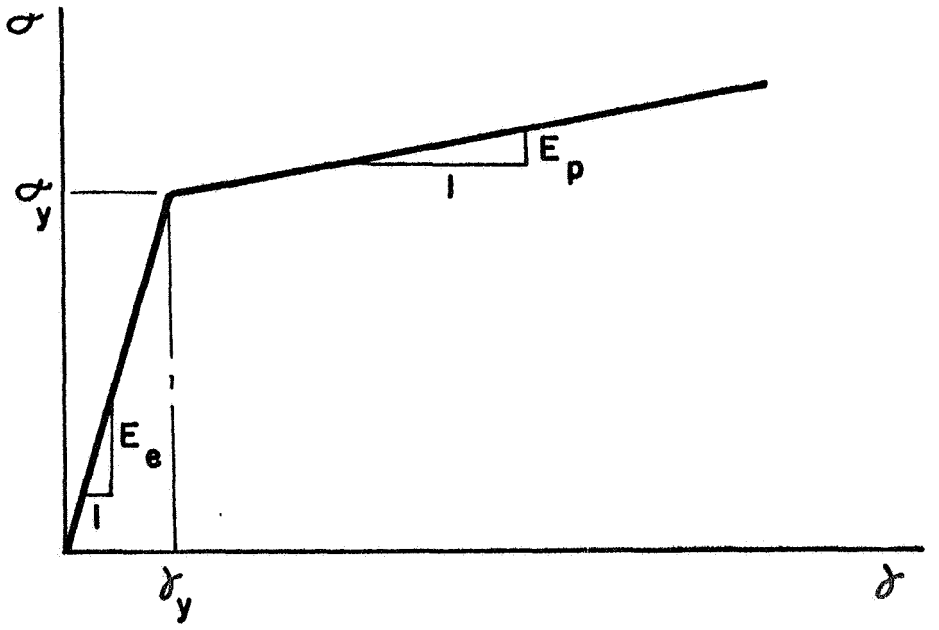

FIG. 6 Bilinear stress-strain law.

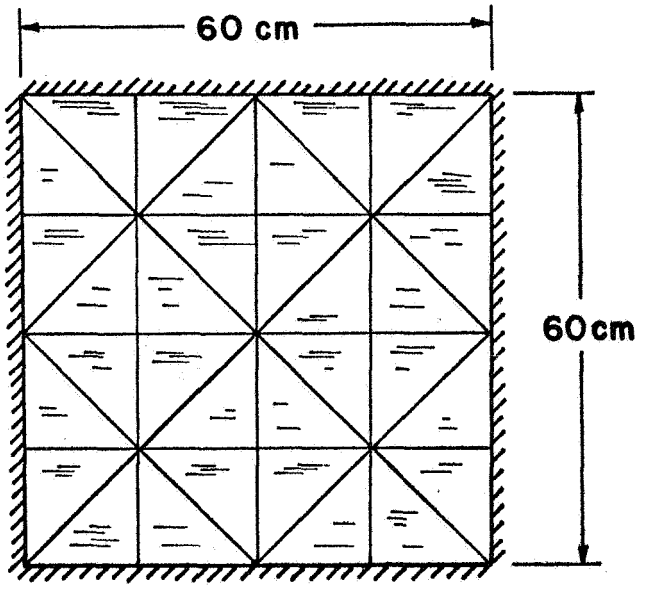

FIG. 7 Finite-element representation of a square metallic membrane.

This behavior was analyzed numerically by using the finite element representation shown in Fig. 7. Figure 8 shows the computed variation in the center displacement of the sheet with external pressure compared with the experimental results of Neubert and Sommer [29] and with results obtained using approximate theories proposed by Foppl [30] and Hencky [31]. Again note that the rather coarse network was adequate to obtain displacements in excellent agreement with experimental data.

6.3 Finite Stretching of a Rubber Sheet. In order to indicate the rate of convergence of the results as the finite-element network is refined, we reproduce here results similar to those obtained earlier by Oden and Sato [11]. In this example, an initially square rubber sheet, 0.127 cm. thick, is stretched in its plane to twice its original length. The material is assumed to be of the Mooney type, with material constants C_1 and C_2 of 1.75 and 0.15 kg/cm^2 respectively. Thus, Eqs. (48) are applicable.

Various finite element representations of the sheet are shown in Fig. 9 along with the variations in the total edge force with the total number of finite elements. In this example, the edge force converged monotonically to approximately 16.32 kg.

6.4 Inflation of an Initially Flat Rubber Membrane. In a recent paper, Hart-Smith and Crisp [32] presented experimental data on the inflation of thin rubber membranes. Although these investigators used an exponential form of the strain energy function, sufficient information was given to deduce equivalent Mooney constants for the material used. Specifically, we consider the inflation of an initially flat, circular, synthetic rubber membrane subjected to uniform external pressure. The membrane is initially 50.8 mm. in diameter and 0.2 mm. thick and is held fixed around its edges in a metal clamp.

In the finite element analysis of this membrane, it was assumed that the

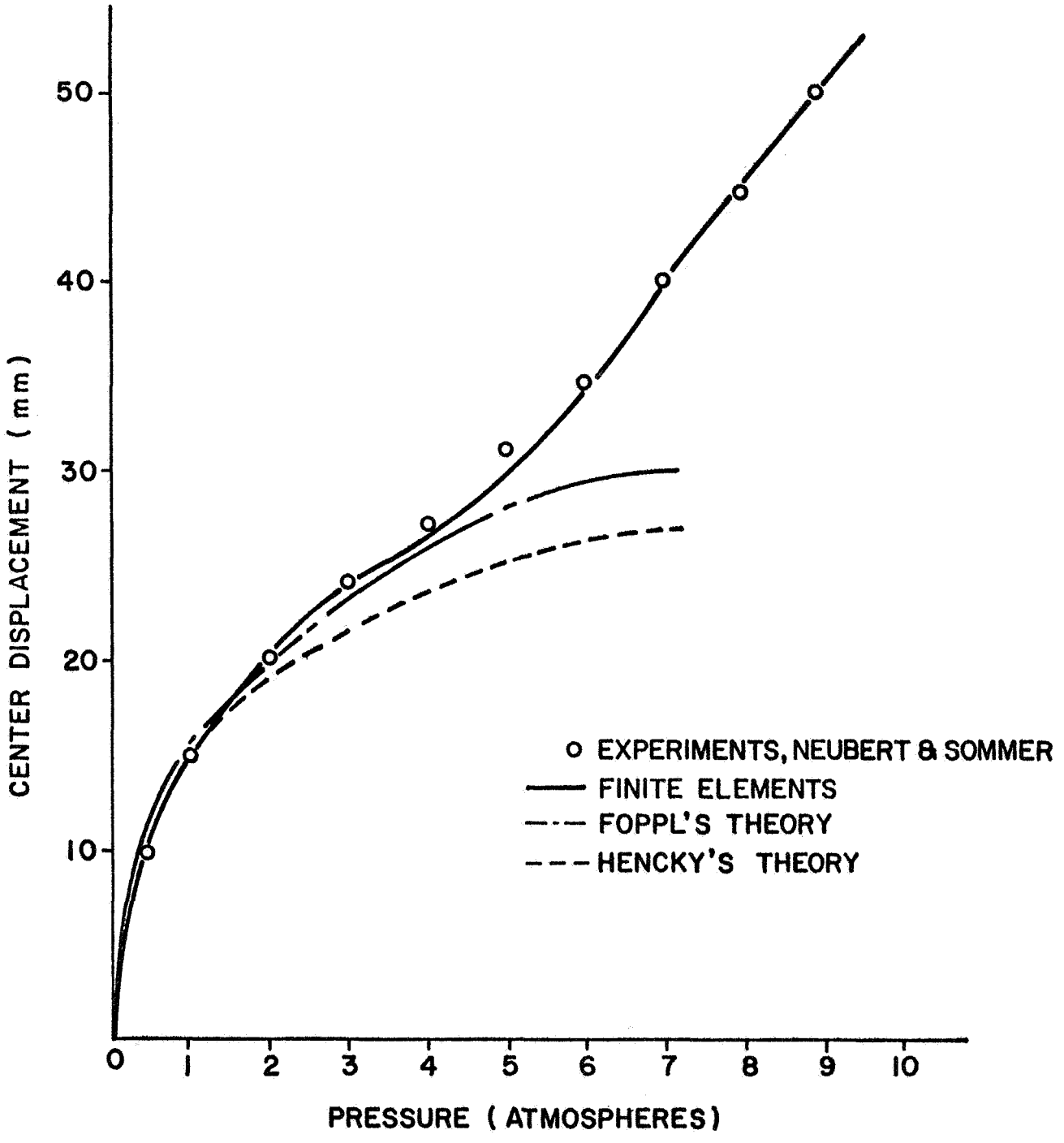

FIG. 8 Variation in center displacement of a square plate with external pressure.

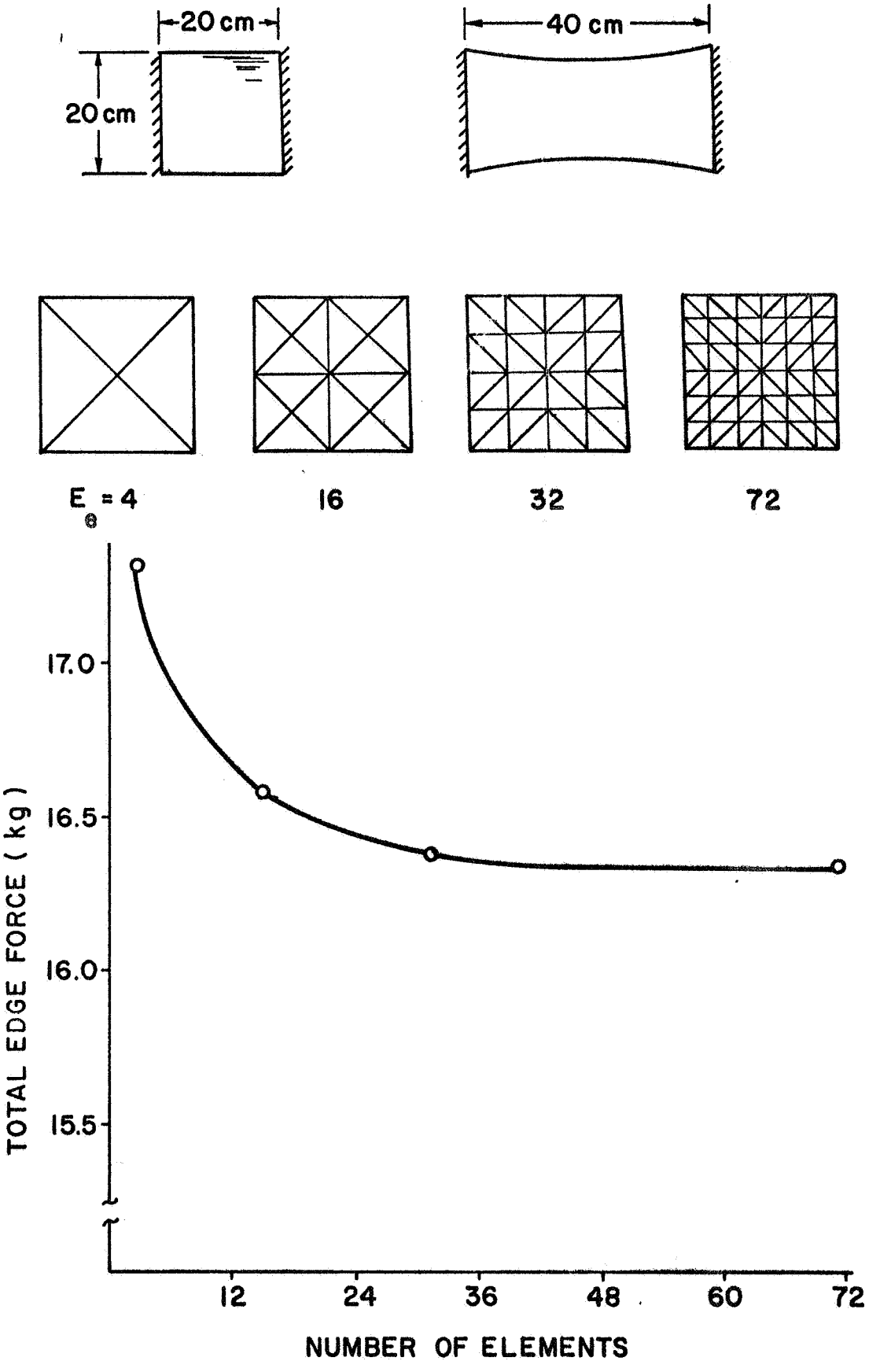

FIG. 9 Finite stretching of a square rubber sheet.

rubber possessed a strain energy function of the Mooney form [Eq.(41)] so that the nonlinear stiffness relations in Eqs. (48) were applicable. Values of the Mooney constants of $C_1 = 9.5C_2 = 1.75$ kg/cm^2 were derived from the data given in [32]. The case considered is that in which the membrane is subjected to a uniform pressure of 0.097 kg/cm^2. According to the experimental data, this corresponds to an extension ratio at the crown of 5.5.

It is important to note that the inflating pressure is a highly nonlinear function of the extension ratio at the crown and, consequently, of the displacements. Thus, more than one equilibrium configuration can exist for a given pressure. No provisions for determining all possible equilibrium states for a specified pressure were incorporated in the present analysis, and the particular configuration obtained depends upon the choice of initial values employed in the iterative solution of the nonlinear stiffness relations.

Several finite element networks were used in the analysis, beginning with a single 30 degree element and eventually using the 10-element representation shown in Fig. 10. For a given finite element network, the rate of convergence of the Newton-Raphson method depends on the choice of initial values of the displacements. Convergence rates are considerably higher for plane problems (such as that in Fig. 9) than in the case of large out-of-plane deformations. In the present example, rates of convergence were increased by first analyzing a coarse finite-element representation of the membrane using a small number of iterations. The results were then used as starting values for a more refined representation, the displacements of the added node points being obtained through linear interpolation.

Figure 11 shows the computed profile of the inflated sheet compared with the profiles obtained experimentally and theoretically by Hart-Smith and Crisp. We observe that the agreement is quite good, the maximum difference

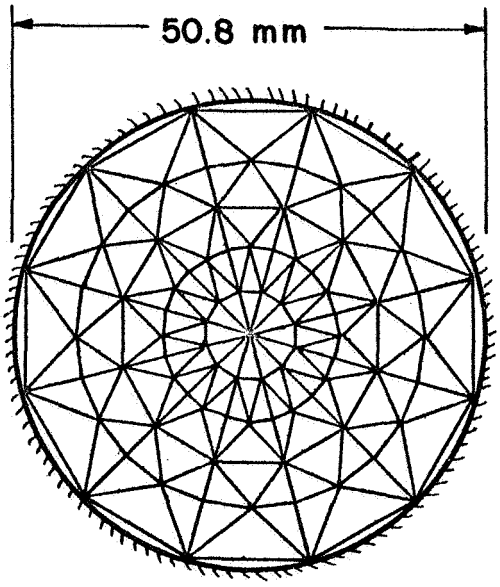

(a)

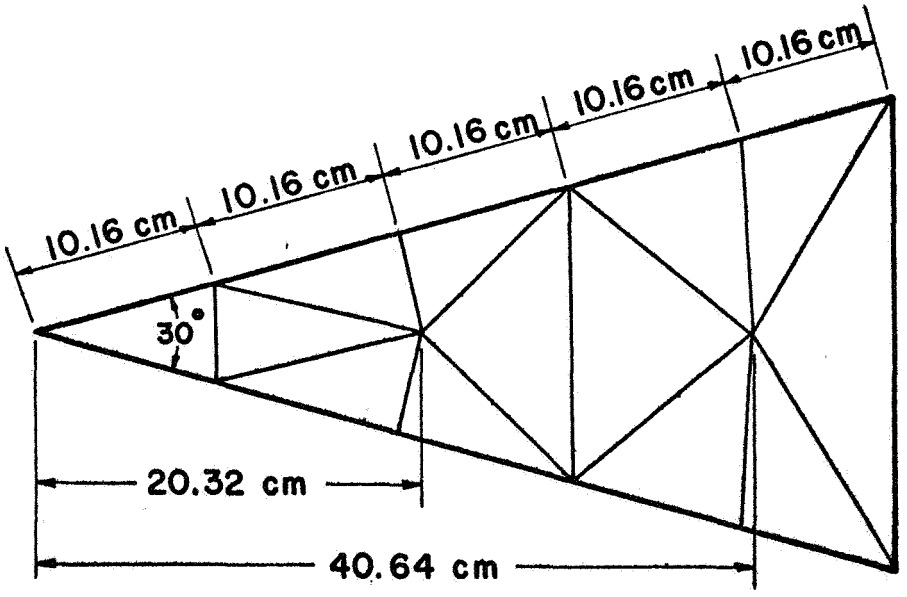

(b)

FIG. 10 (a) Finite-element representation of a circular membrane and (b) a typical 30° segment.

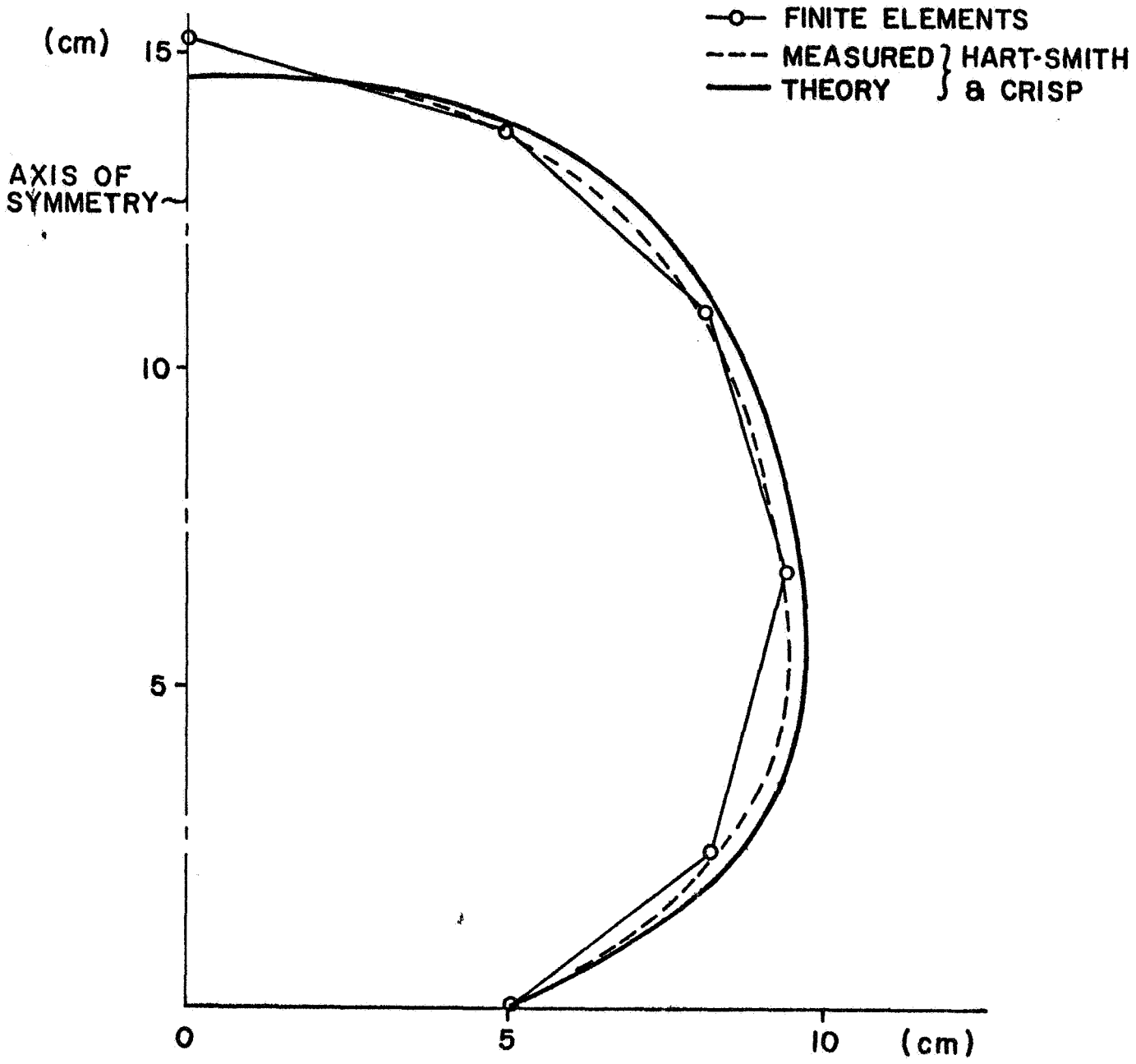

FIG. 11 Comparison of inflated profiles calculated by the finite-element method with profiles obtained experimentally and theoretically by Hart-Smith and Crisp [32].

between the displacements computed by the finite-element analysis and the experimental values being approximately six per cent.

6.5 Experiments on Rubber Membranes. As a final example, we consider briefly the results of experiments performed at the Structures and Materials Laboratory of the University of Alabama Research Institute on thin natural rubber membranes. In these experiments, circular disks, 0.0068 inc. (0.0173 cm.) thick and 15.0 in. (38.1 cm.) in diameter, of pure gum natural rubber sheet were clamped around their edges in a metal clamp. The disks were marked at the center and on ten equally spaced concentric circles. The disks were then inflated in stages of pressures of approximately 100 mm. of water, which corresponded to a polar extension ratio of around $\lambda = 5$. After resisting maximum pressures for 45 minutes, the specimens were then deflated in stages until all applied pressure was removed.

Figure 12 shows the experimental apparatus and a typical inflated circular membrane. Figure 13 indicates the variation in polar extension ratio with pressure. It is seen that the behavior is highly nonlinear and that some energy is dissipated in the unloading process. A residual extension at the center of approximately $\lambda = 1.25$ was experienced, which was completely recovered within 24 hours after unloading.

A finite element representation with 96 elements, four nodes along 30° radial lines was used to determine the inflated profile of a typical specimen subjected to a pressure of 61 mm. of water. Again, the material was assumed to be of the Mooney type, with constants $C_1 = 1.14\ kg/cm^2$ and $C_2 = 0.14\ kg/cm^2$ determined by the method of Hart-Smith and Crisp [32] and data in Figure 13. No attempt was made to predict the obvious viscoelastic character of the behavior. Results of these calculations are given in Fig. 14.

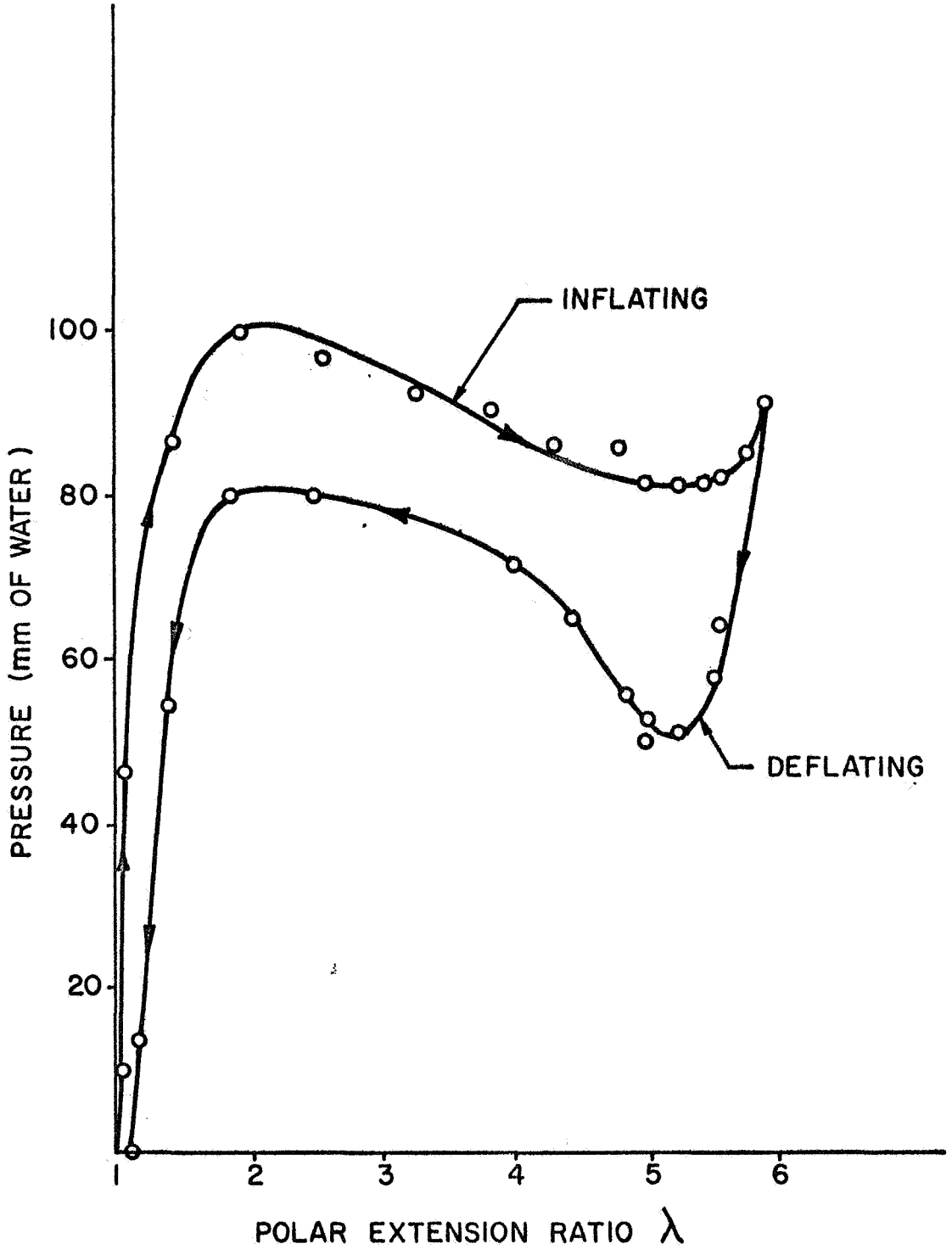

FIG. 13 Variation in polar extension ratio with internal pressure.

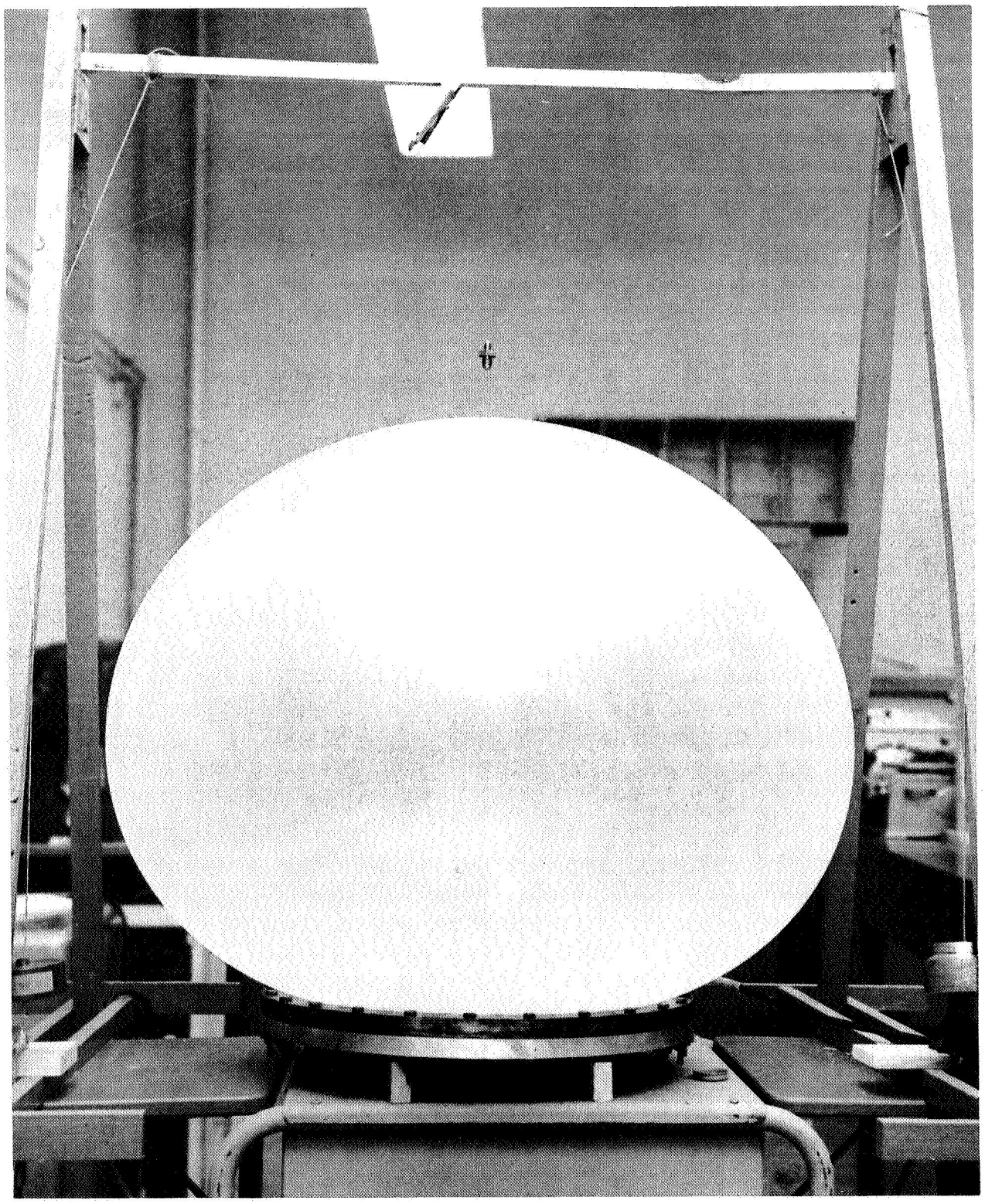

Fig. 12 Inflated membrane used in experiments.

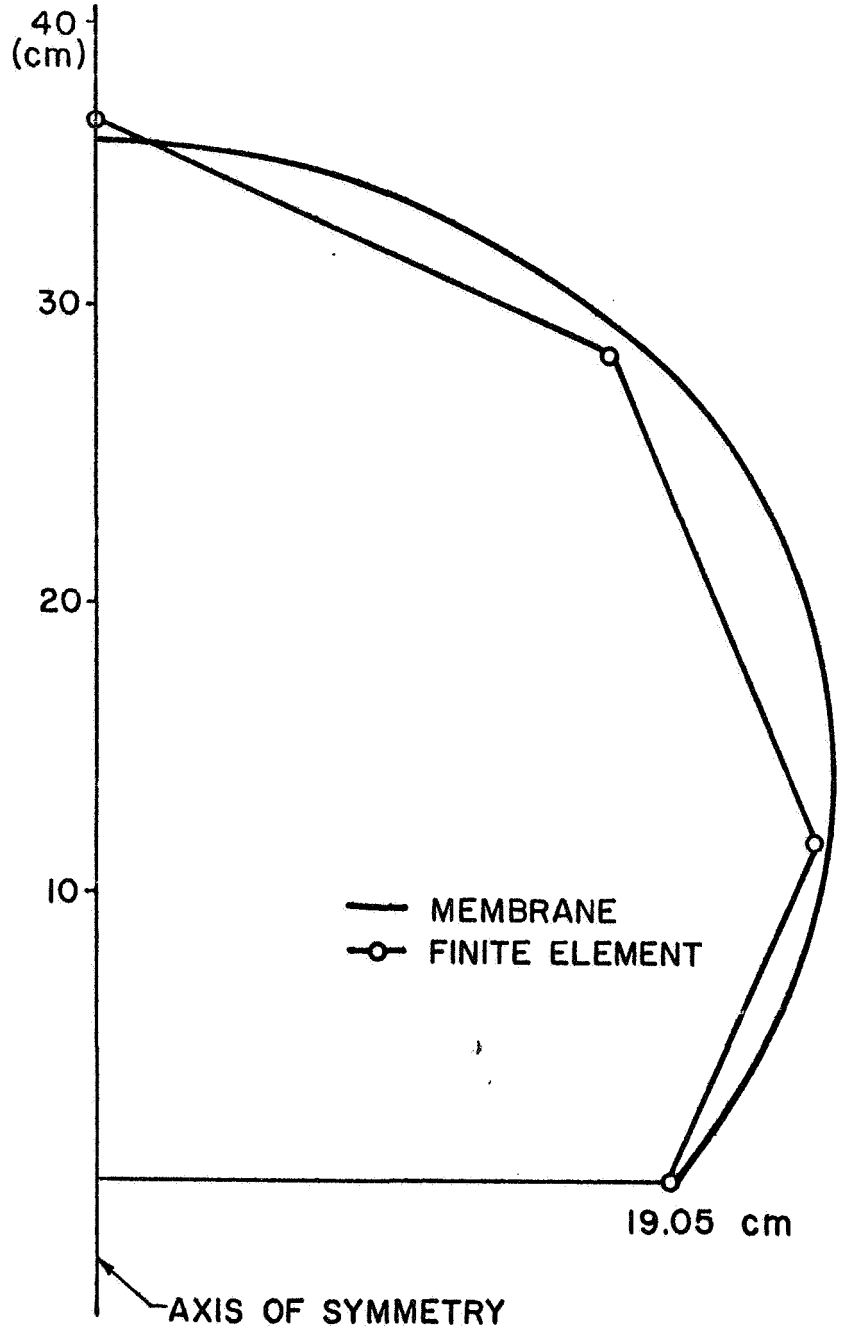

FIG. 14 Comparison of measured profile of an inflated rubber disk with profile obtained from finite element analysis.

ACKNOWLEDGMENT

It is a pleasure to acknowledge the assistance of Mr. T. Sato, who developed the computer programs used in all of the calculations. This work was supported by the National Aeronautics and Space Administration through General Research Grant NsG-381, and the synthetic rubber materials used in the experiment were donated by the Materials Laboratory of NASA's Marshall Space Flight Center.

REFERENCES

1. TURNER, M. J., DILL, E. H., MARTIN, H. C., and MELOSH, R. J., "Large Deflections of Structures Subjected to Heating and External Loads," Journal of the Aero/Space Sciences, Vol. 27, February 1960, pp. 97-106.

2. ARGYRIS, J. H., "Recent Advances in Matrix Methods of Structural Analysis," Progress in Aeronautical Sciences, Pergamon Press, Oxford, England, 1964, pp. 115-133.

3. ARGYRIS, J. H., "Matrix Analysis of Three-Dimensional Elastic Media-Small and Large Displacements," AIAA Journal, Vol. 3, No. 1, January 1965, pp. 45-51.

4. GALLAGHER, R. H. and PADLOG, J., "Discrete Element Approach to Structural Instability Analysis," AIAA Journal, Vol. 1, No. 6, June 1963, pp. 1437-1439.

5. MARTIN, H. C., "On the Derivation of Stiffness Matrices for the Analysis of Large Deflection and Stability Problems," Conference on Matrix Methods in Structural Mechanics, Wright-Patterson AFB, Dayton, Ohio, October 1965.

6. ODEN, J. T., "Calculation of Geometric Stiffness Matrices for Complex Structures," AIAA Journal, Vol. 4, No. 6, August 1966, pp. 1480-1482.

7. WISSMANN, J. W., "Numerische Berechnung nichtlinear elastischer Koerper," Dissertation, Hannover, 1963.

8. WISSMANN, J. W., "Nonlinear Structural Analysis; Tensor Approach," Conference on Matrix Methods in Structural Mechanics, Wright-Patterson AFB, Dayton, Ohio, October 1965.

9. ODEN, J. T., "Analysis of Large Deformations of Elastic Membranes by the Finite Element Method," Proceedings, IASS Congress on...Large Span Shells, Leningrad, September, 1966.

10. ODEN, J. T., "Numerical Formulation of Nonlinear Elasticity Problems," Journal of the Engineering Mechanics Division, ASCE, June 1967.

11. ODEN, J. T. and SATO, T., "Finite Strains and Displacements of Elastic Membranes by the Finite Element Method," International Journal of Solids and Structures, June 1967.

12. BECKER, E. B., "A Numerical Solution of a Class of Problems of Finite Elastic Deformation," Dissertation, University of California, Berkeley, California, 1966.

13. GREEN, A. E. and ADKINS, J. E., Large Elastic Deformations and Non-linear Continuum Mechanics, Oxford University Press, London, 1960.

14. ERINGEN, A. C., Nonlinear Theory of Continuous Media, McGraw Hill Book Co., New York, 1962.

15. RIVLIN, R. S. and SAUNDERS, D. W., "Large Elastic Deformations of of Isotropic Materials. VII Experiments on the Deformation of Rubber," Philosophy Transactions of the Royal Society, No. 243, London, 1951, pp. 251-288.

16. RIVLIN, R. S. and SAUNDERS, D. W., "The Free Energy of Deformation for Vulcanized Rubbers," Transactions of the Faraday Society, No. 48, 1952, pp. 200-206.

17. MOONEY, M., "A Theory of Large Elastic Deformations," Journal of Applied Physics, No. 11, 1940, pp. 582-592.

18. TRELOAR, L. R. G., The Physics of Rubber Elasticity, 2nd Edition, Oxford University Press, London, 1958.

19. RIVLIN, R. S., "Large Elastic Deformations of Isotropic Materials. I Fundamental Concepts," Philosophy Transactions of the Royal Society, No. 240, London, 1948, pp. 459-490.

20. HUTCHINSON, W. D., BECKER, G. W., and LANDEL, R. F., "Determination of the Stored Energy Function of Rubber-like Materials," Bulletin, Fourth Meeting of CPIA Working Group on Mechanical Behavior, 1965.

21. BORESI, A. P., LANGHAAR, H. L. and MILLER, R. E., "Buckling of Axially-Compressed Bilayered Fiber-Reinforced Elastic Cylindrical Shell," Developments in Theoretical and Applied Mechanics. Vol. 2, Proceedings of the Second Southeastern Conference on Theoretical and Applied Mechanics, W. A. SHAW Ed., Pergamon Press, London, 1965, pp. 95-115.

22. POPE, G. G., "The Application of the Matrix Displacement Method in Plane Elasto-Plastic Problems," Conference on Matrix Methods in Structural Mechanics, Wright-Patterson AFB, Dayton, Ohio, October 1965.

23. POPE, G. G., "A Discrete Element Method for the Analysis of Plane Elastoplastic Stress Problems," The Aeronautical Quarterly, February 1966.

24. HILL, R., The Mathematical Theory of Plasticity, Oxford University Press, London, 1950.

25. REMMLER, K. L., CAWOOD, D. W., STANTON, J. A., and HILL, R., "Solutions of Systems of Nonlinear Equations," Lockheed MSC/HREC, NASA 8-20178, October 1966.

26. SPRANG, H. A., "A Review of Minimization Techniques for Nonlinear Functions," SIAM Review, Vol. 4, No. 4, October 1962, pp. 343-364.

27. BROOKS, S. H., "A Comparison of Maximum Seeking Methods," Journal of Operations Research, Vol. 7, 1959, pp. 430-457.

28. KUHN, P., Stresses in Aircraft Structures, McGraw-Hill Book Co., New York, 1956, pp. 105-110.

29. NEUBERT, M. and SOMMER, A., "Rechteckige Blechhaut unter gleichmässig verteiltem Flusigkeitsdruck," Luftfahrtforschung, Vol. 17, No. 7, July 20, 1940, pp. 207-210 (also published as NACA Technical Memorandu, 965, December 1940).

30. FOPPL, A. and FOPPL, L., Drang und Zwang, Vol. 1, Oldenbourg, 1924.

31. HENCKY, H., "Die Berechnung dünner rechteckiger Platten mit verschwindender Biegungsteifigkeit," Zeitschrift für Angewandte Mathematik und Mechanik, (ZAMM), Bd. 1, Heft 2, April 2, 1921, pp. 81-89.

32. HART-SMITH, L. J. and CRISP, J. D. C., "Large Elastic Deformations of Thin Rubber Membranes," International Journal of Engineering Science, Vol. 5, No. 1, January 1967, pp. 1-24.